SAND2020-1712PE

Sandia National Laboratories

Exceptional service in the national interest

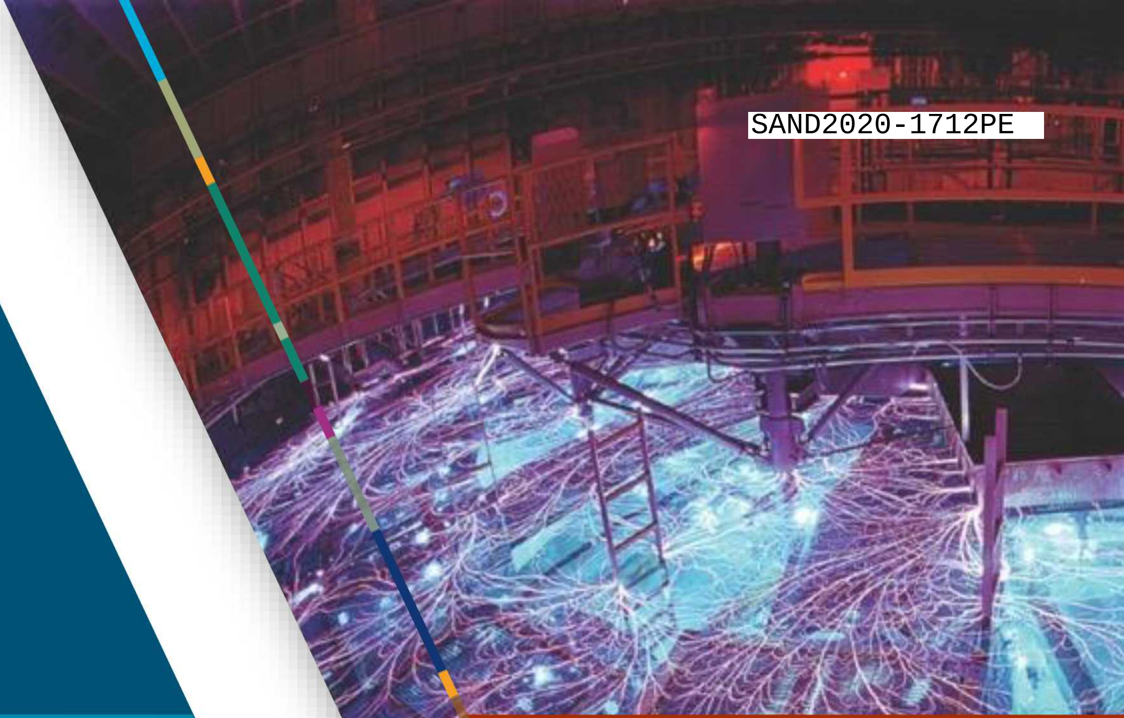

Integrated Geomechanics and Geophysics in Induced Seismicity: Experiments of Geo-architected Rocks and Machine Learning Applications

Hongkyu Yoon
Geomechanics Department
Sandia National Laboratories, NM

ENERGY NNSA

Sandia National Laboratories is a multimission laboratory managed and operated by National Technology and Engineering Solutions of Sandia LLC, a wholly owned subsidiary of Honeywell International Inc. for the U.S. Department of Energy's National Nuclear Security Administration under contract DE-NA0003525.

Acknowledgments

- Laboratory Directed Research and Development program at Sandia National Laboratories

- U.S. DOE, Office of Fossil Energy, Fossil Energy Research and Development Program

Collaborators:
Daniel Lizama, K-Won Chang (Sandia)
Laura Pyrak-Nolte, Antonio Bobet, Liyang Jiang (Purdue Univ.)

Abstract

Quantifying in-situ subsurface stresses and predicting fracture development are critical to reducing risks of induced seismicity and improving modern energy activities in the subsurface. In this work, we developed a novel integration of controlled mechanical failure experiments coupled with microCT imaging, acoustic sensing, modeling of fracture initiation and propagation, and machine learning for event detections and waveform characterization. Through additive manufacturing (3D printing), we were able to produce bassanite-gypsum rock samples with repeatable physical, geochemical and structural properties. With these “geo-architected” rock, we provided the role of mineral texture orientation on fracture surface roughness. The impact of poroelastic coupling on induced seismicity has been systematically investigated to improve mechanistic understanding of post shut-in surge of induced seismicity. This research will set the groundwork for characterizing seismic waveforms by using multiphysics and machine learning approaches and improve the detection of low-magnitude seismic events leading to the discovery of hidden fault/fracture systems.

SANDIA NATIONAL LABORATORIES OVERVIEW

SANDIA'S HISTORY IS TRACED TO THE MANHATTAN PROJECT

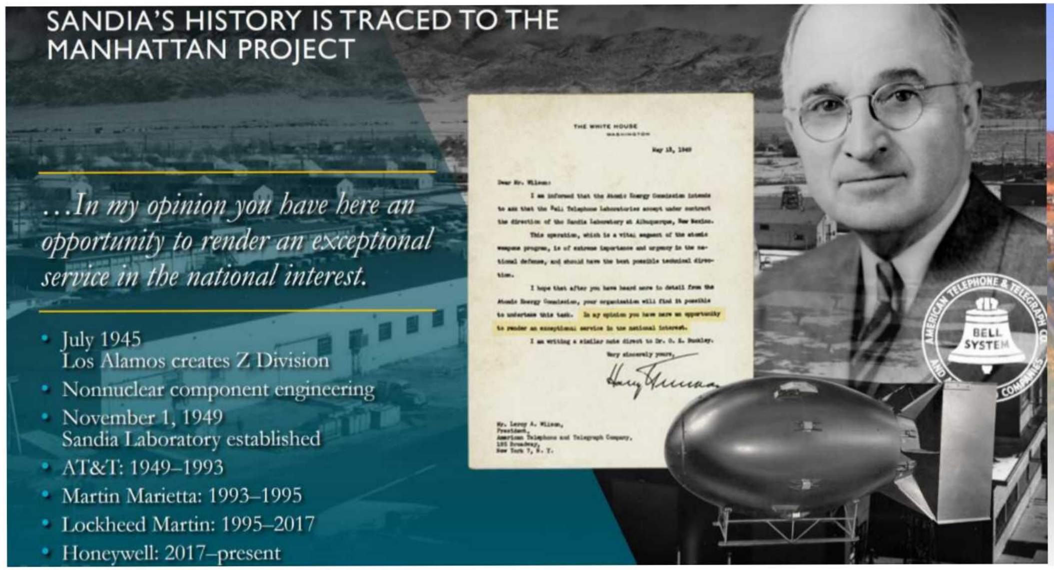

...In my opinion you have here an opportunity to render an exceptional service in the national interest.

- July 1945
  Los Alamos creates Z Division
- Nonnuclear component engineering
- November 1, 1949
  Sandia Laboratory established
- AT&T: 1949–1993
- Martin Marietta: 1993–1995
- Lockheed Martin: 1995–2017
- Honeywell: 2017–present

SANDIA HAS FACILITIES ACROSS THE NATION

Activity locations

- Kauai, Hawaii
- Waste Isolation Pilot Plant, Carlsbad, New Mexico
- Pantex Plant, Amarillo, Texas
- Tonopah, Nevada

Main sites

- Albuquerque, New Mexico
- Livermore, California

SANDIA ADDRESSES NATIONAL SECURITY CHALLENGES

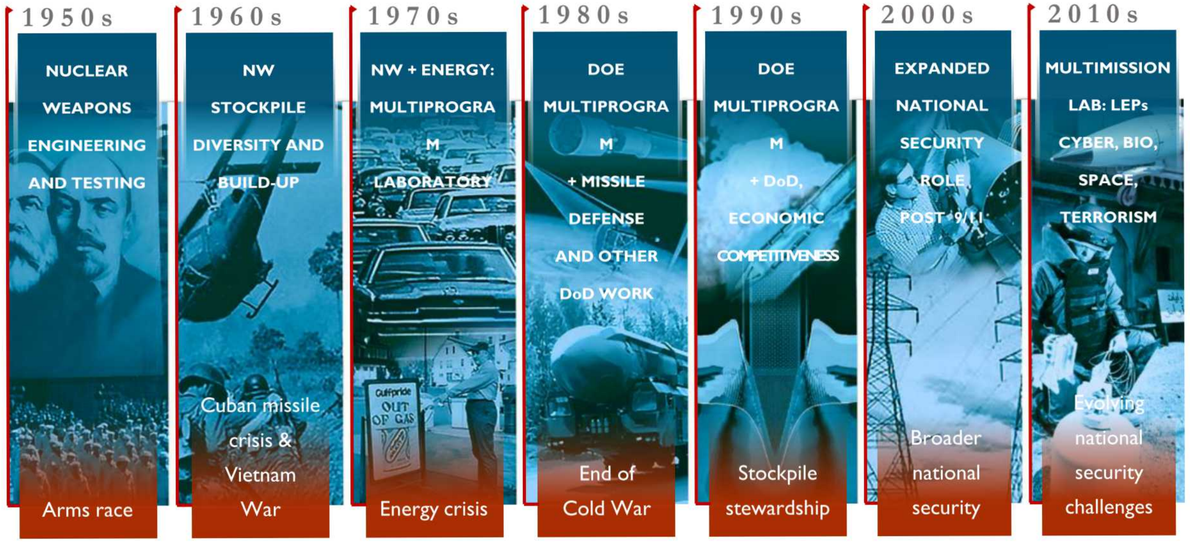

1950s	1960s	1970s	1980s	1990s	2000s	2010s
NUCLEAR WEAPONS ENGINEERING AND TESTING	NW STOCKPILE DIVERSITY AND BUILD-UP	NW + ENERGY: MULTIPROGRAM LABORATORY	DOE MULTIPROGRAM + MISSILE DEFENSE AND OTHER DoD WORK	DOE MULTIPROGRAM + DoD, ECONOMIC COMPETITIVENESS	EXPANDED NATIONAL SECURITY ROLE POST 9/11	MULTIMISSION LAB: LEPs CYBER, BIO, SPACE, TERRORISM
Arms race	Cuban missile crisis & Vietnam War	Energy crisis	End of Cold War	Stockpile stewardship	Broader national security	Evolving national security challenges

SANDIA'S BUDGET and WORKFORCE

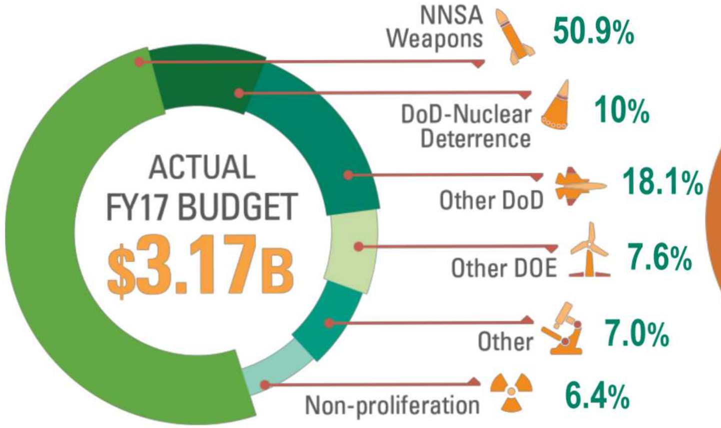

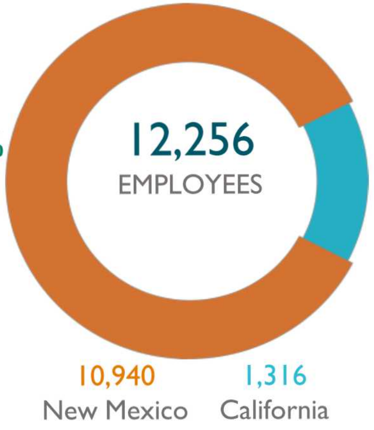

Geoscience Research & Applications

Yucca Mountain Project

Waste Isolation Pilot Plant

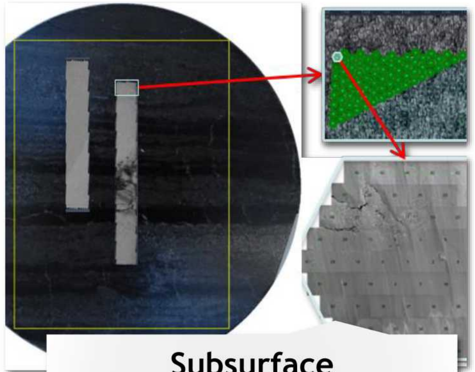

Subsurface Characterization & Engineering

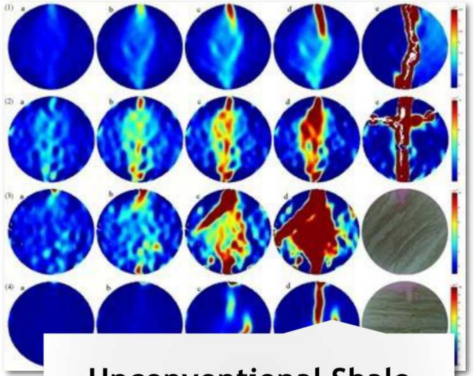

Unconventional Shale Science

National Emergency Responses

Columbia Accident, 2003
Deep Water Horizon, 2010
Aliso Canyon Gas Leak, 2015

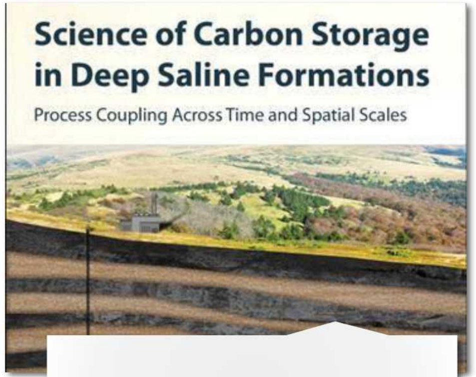

CO_2 Sequestration

Drilling Technology & Downhole Tools

Strategic Petroleum Reserve

Safe Oil & Gas Transport

- **Motivations**
- Mechanical testing of Geo-architected rocks
- Machine learning applications at laboratory scale
- Machine learning applications at field scale
- Geological CO_2 storage
- Unconventional resources & recovery

Background & Motivations

♦ Motivations

- Fluid injection or withdrawal causes changes in pore pressure, resulting in induced seismicity during subsurface energy activities
- Reduce risks of induced seismicity and improve subsurface energy activities (unconventional resource recovery, geological carbon storage, geothermal energy recovery)

Induced (human-caused) seismicity

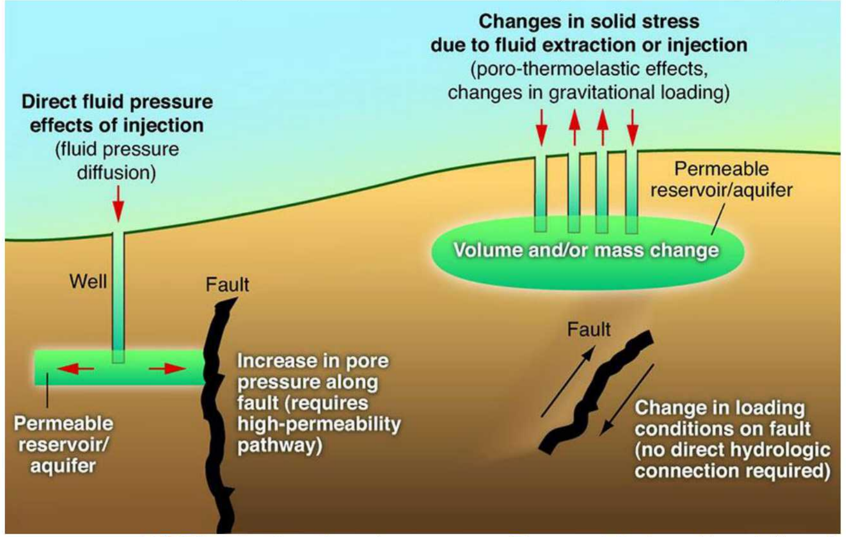

USGS: http://earthquake.usgs.gov/Research/induced/modeling.php

♦ Goals

(1) Delineate fracture and failure mechanisms using well-controlled experiments

(2) Determine poro-elastic coupling mechanisms that lead to induced seismicity during fluid injection into subsurface (Chang et al., 2018; Chang and Yoon (2018))

(3) Develop/apply machine-learning techniques for seismic wave data analysis and event detection

♦ Approaches

An ambitious integration of controlled mechanical failure experiments coupled with micro-CT imaging, acoustic sensing, modeling of fracture initiation and propagation, and machine learning for event detections and waveform characterization

Linkage between geomechanical and geophysical processes in mechanical discontinuities

- Precursor(s) to the induced seismicity from existing fault/fracture systems is key
- Changes in the spectral contents of waveforms are likely due to wave propagation + faulting processes - initiation, propagation and coalescence of pre-existing discontinuities loaded in mixed mode I-II-III (**Damage Mechanics Challenge, AGU 2019 session**)

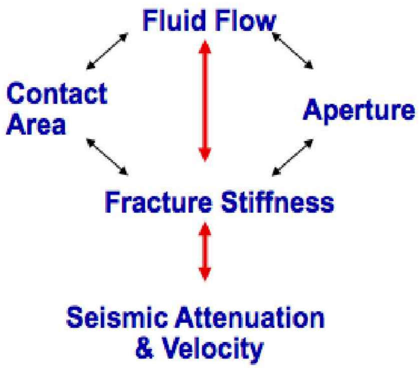

Courtesy from Pyrak-Nolte

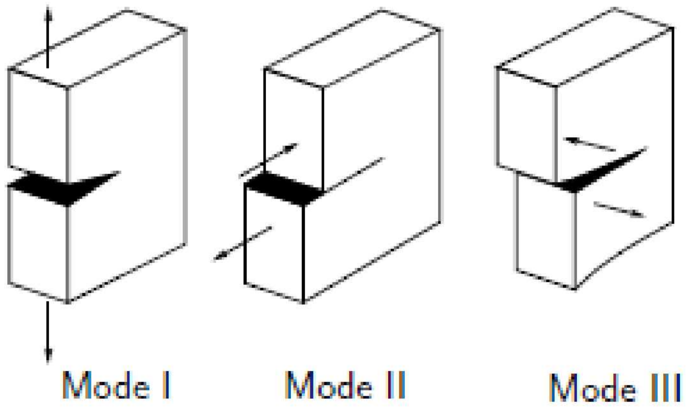

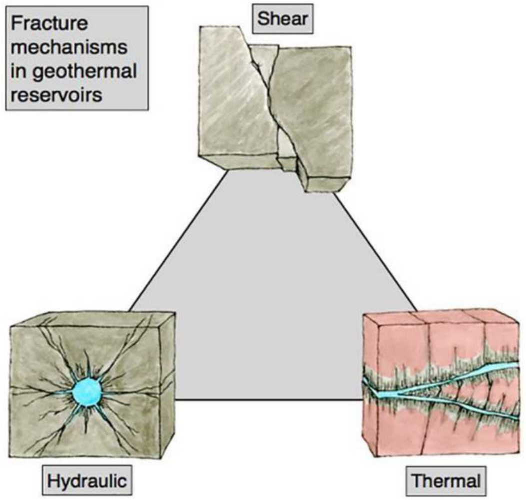

Holtzman et al. Sci Adv 2018

Precursors to Slip along a Mechanical Discontinuity

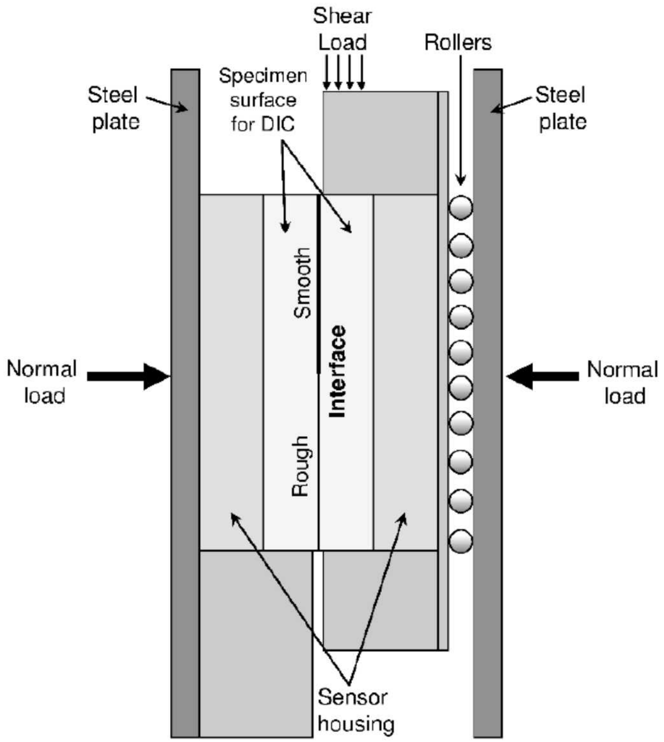

Bi-axial testing

(Hedayat et al, 2014)

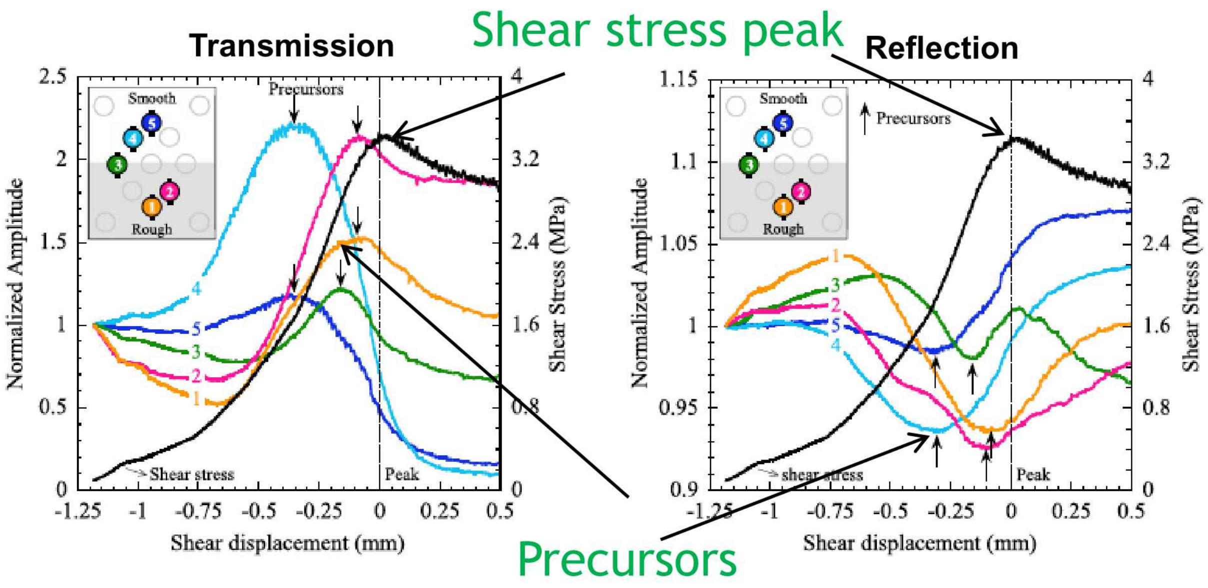

► Increase in transmitted shear wave amplitude prior to achieving the peak shear stress

► Post pre-peak seismic response depends on the frictional characteristics of the interface

Need to determine how these results apply in a more realistic setting with spatial and temporal variations in pre-existing discontinuities, stress and pressure fields, fluid migration and rock types

- Motivations
- **Mechanical testing of Geo-architected rocks**
- Machine learning applications at laboratory scale
- Machine learning applications at field scale
- Geological CO_2 storage
- Unconventional resources & recovery

Integrated approach for geomechanical and geophysical measurements

Geo-architected Rock

Mechanical testing (3PB) & Signals Prior to Failure

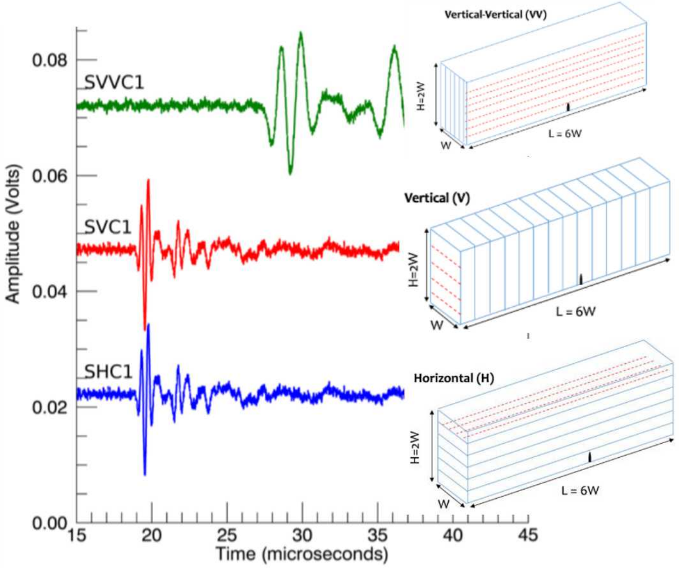

MicroCT imaging

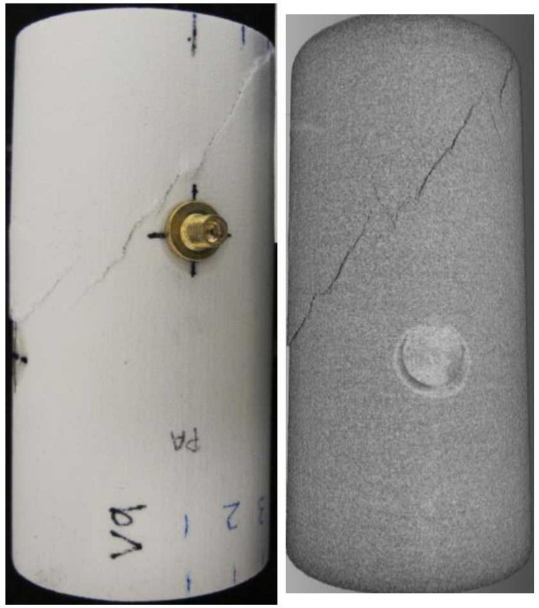

Waveform data analysis

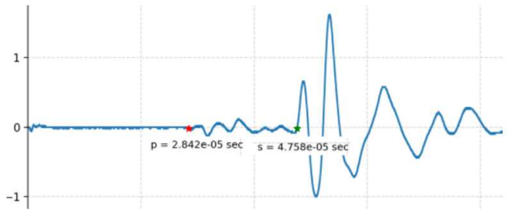

3PB experiments and simulations

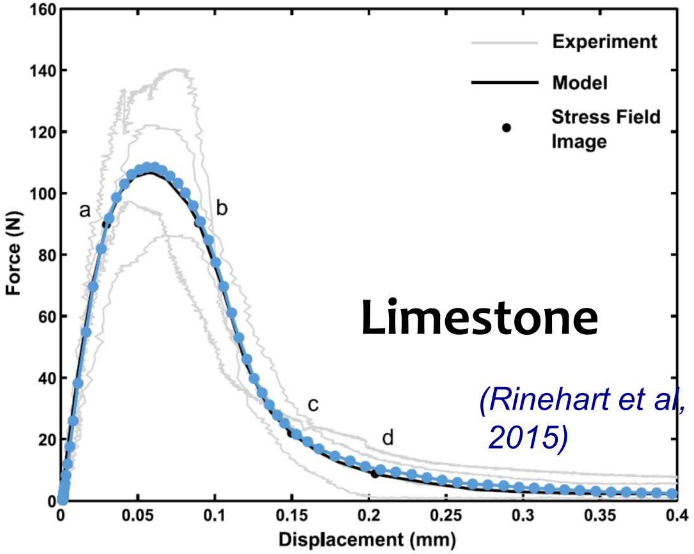

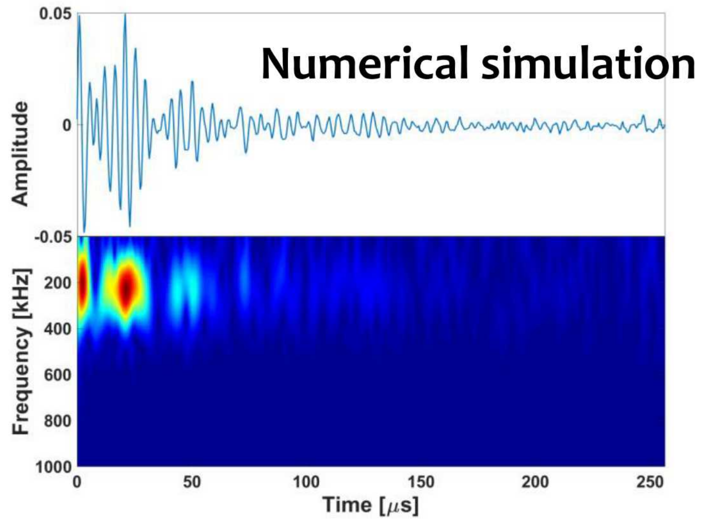

Powder Based 3D Printing Process

$$CaSO_4 \cdot 0.5H_2O + 1.5H_2O = CaSO_4 \cdot 2H_2O$$

Powders (basanite) Binder Gypsum

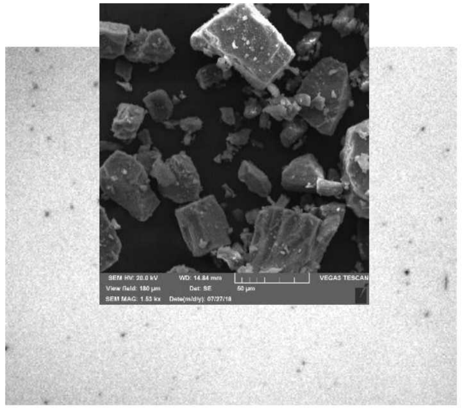

powders

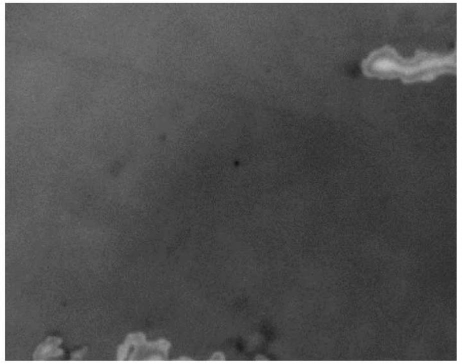

Binder dropped

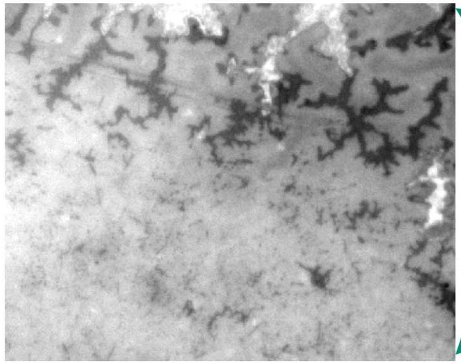

Reaction products

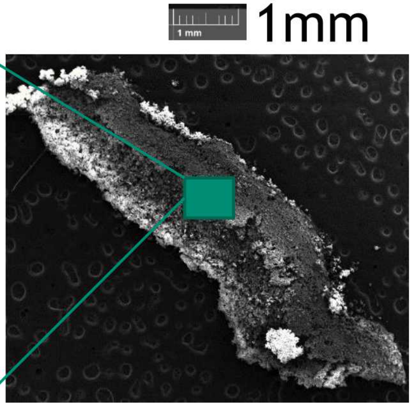

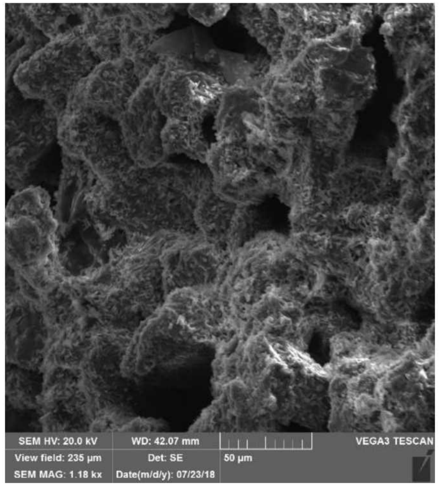

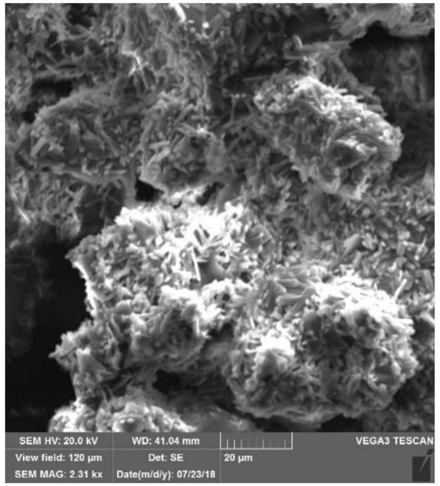

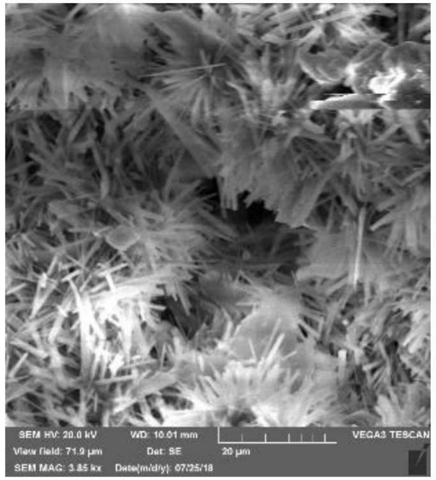

Geo-architected Rock

A geo-architected rock is a rock analog that is fabricated and structured using conventional or unconventional methods to develop controlled features in specimens that promote repeatable experimental behavior.

**Material Properties*

- **Unconfined Compressive Strength Test*
- **Ultrasonic Compressional & Shear Wave Measurements*

**Tensile Failure of Geo-Architected Rock (three point bending test)*

Rock Variability: “Shale”

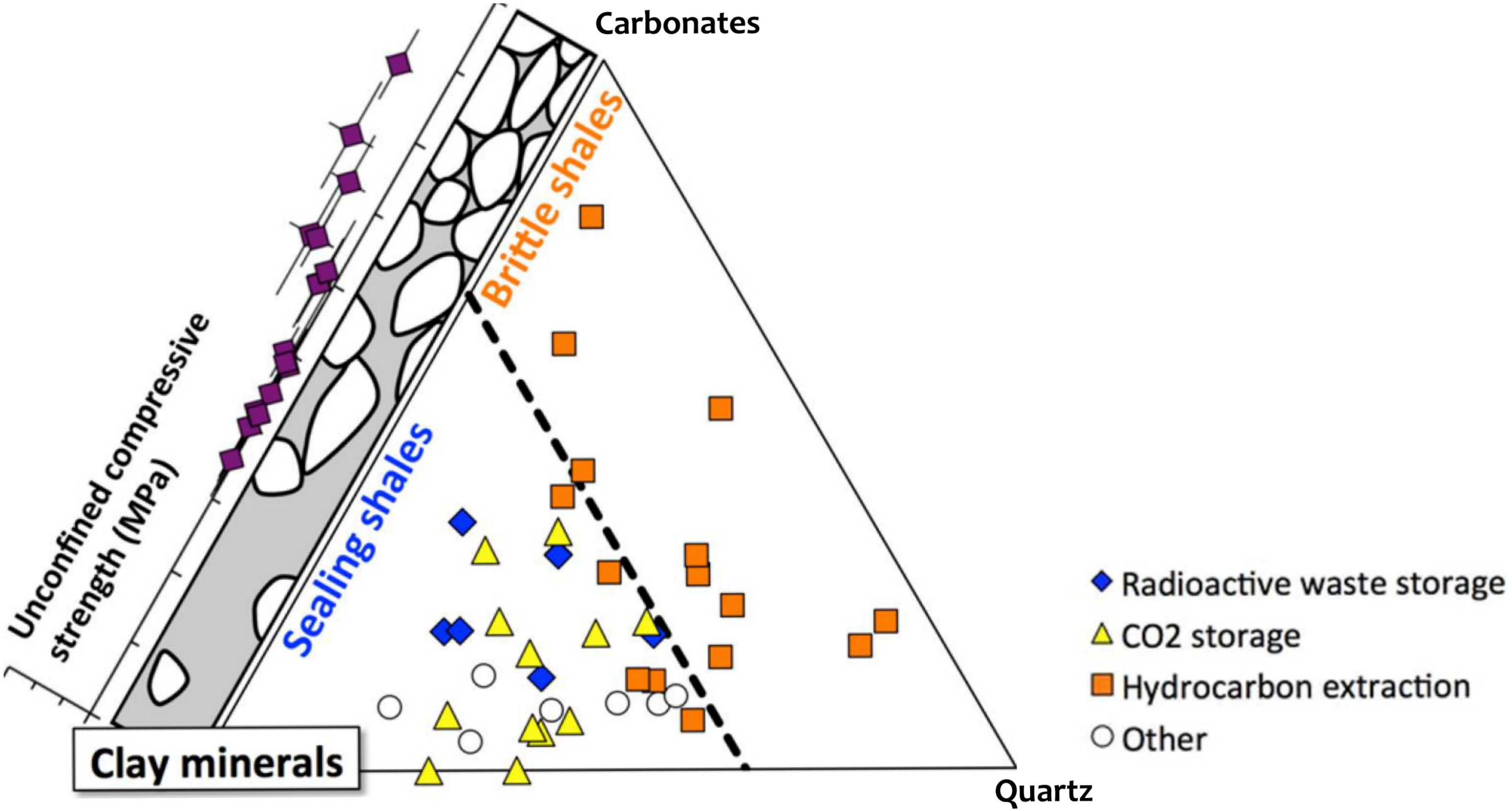

(Bourg et al., 2015)

Observations of Fracture Resistance in Layered Geological Media

A. A thin section of Mancos shale after Indirect tensile testing

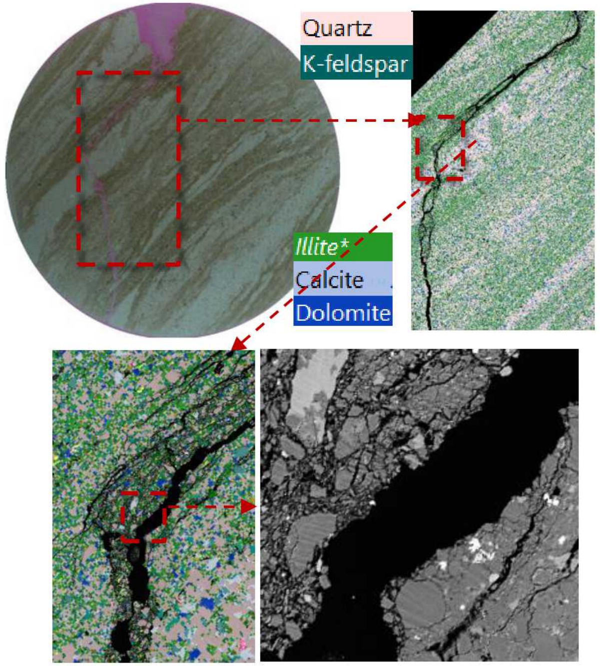

B. Lateral strain based on digital image correlation measurements

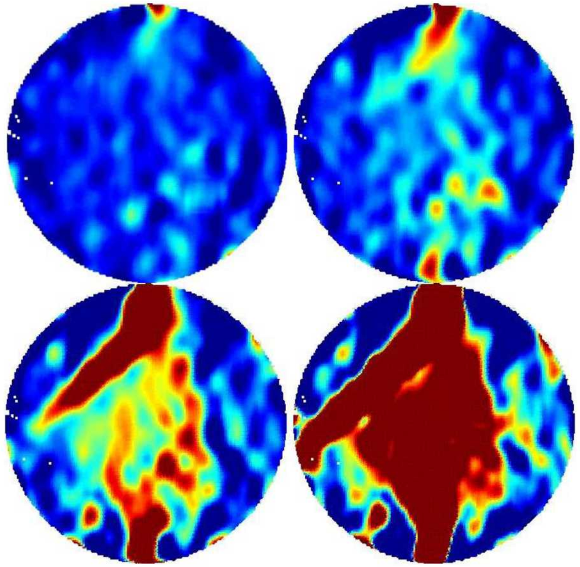

C. Phase field modeling results (crack initiation & propagation)

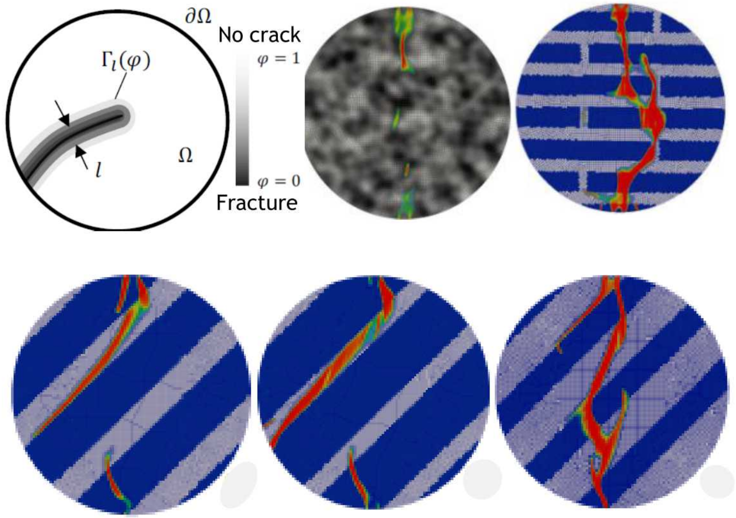

Na et al. (2017, JGR); Yoon et al. (2019, AAPG Memoir 102)

Geo-architected Rock

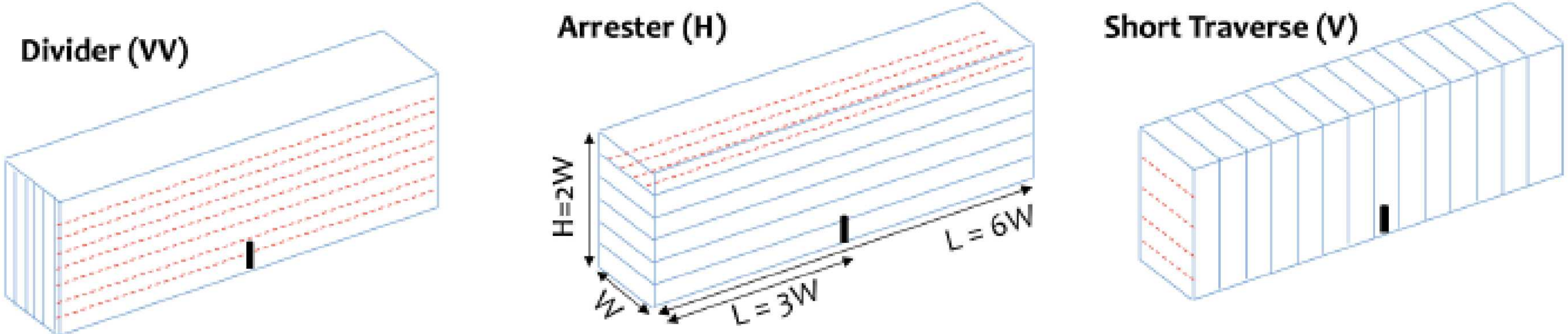

Three Point Bending Experiments: Repeatability

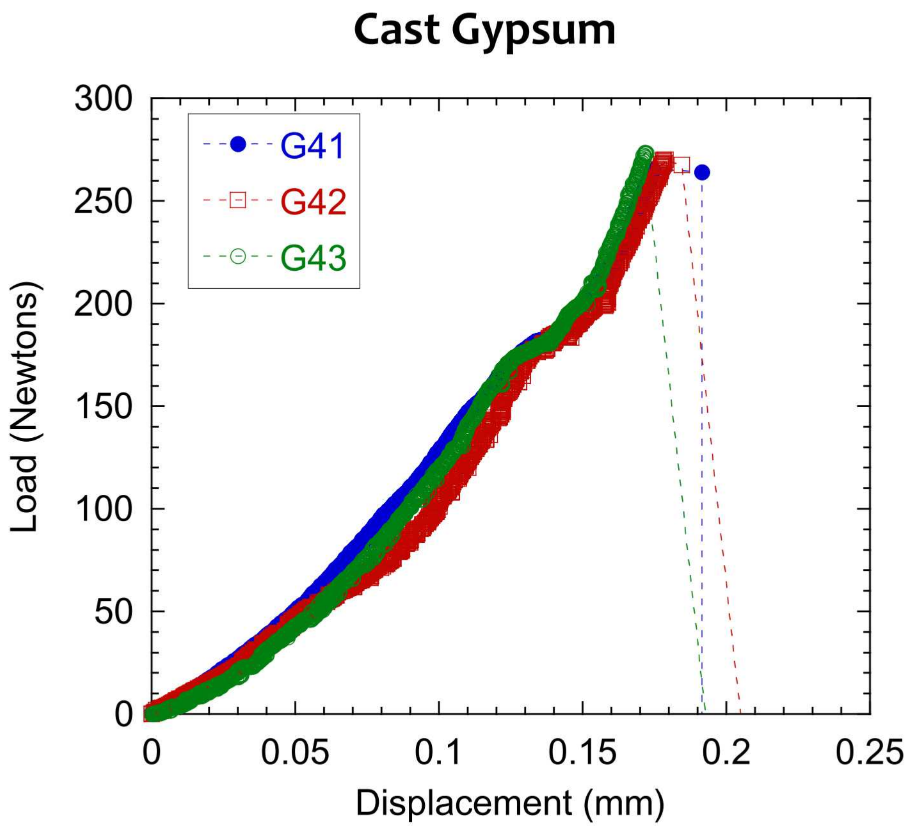

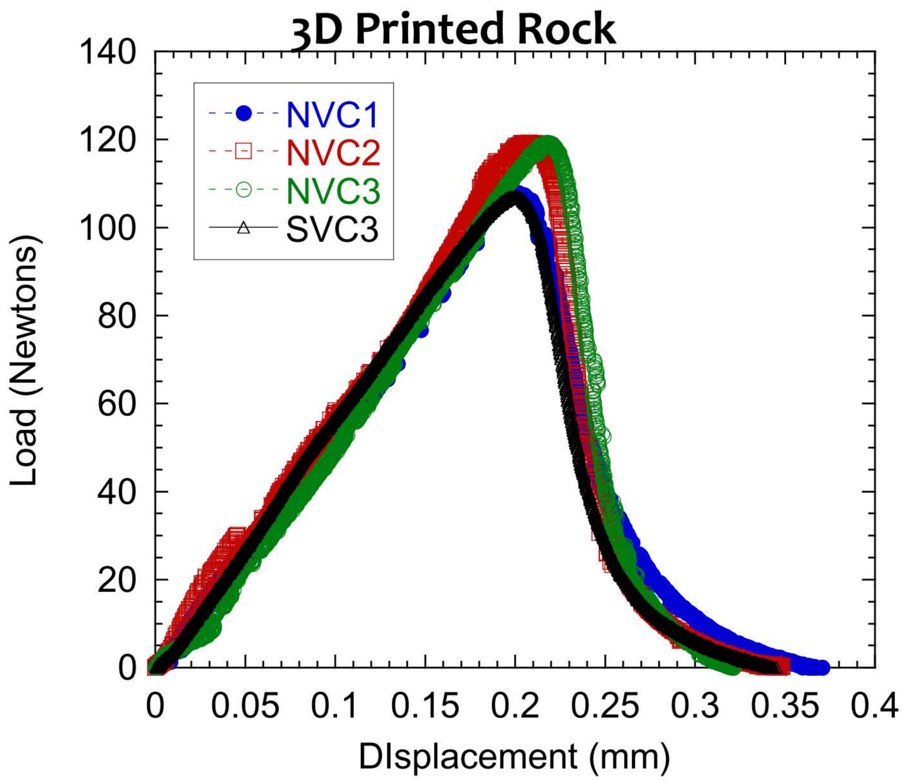

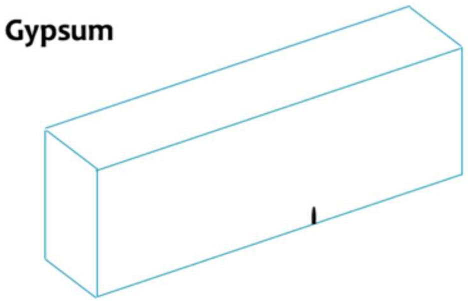

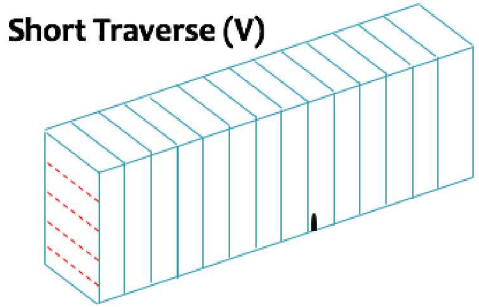

Jiang et al. (Sci Rep 2020, In press)

Observation of Seismic Anisotropy in 3D Printed Samples

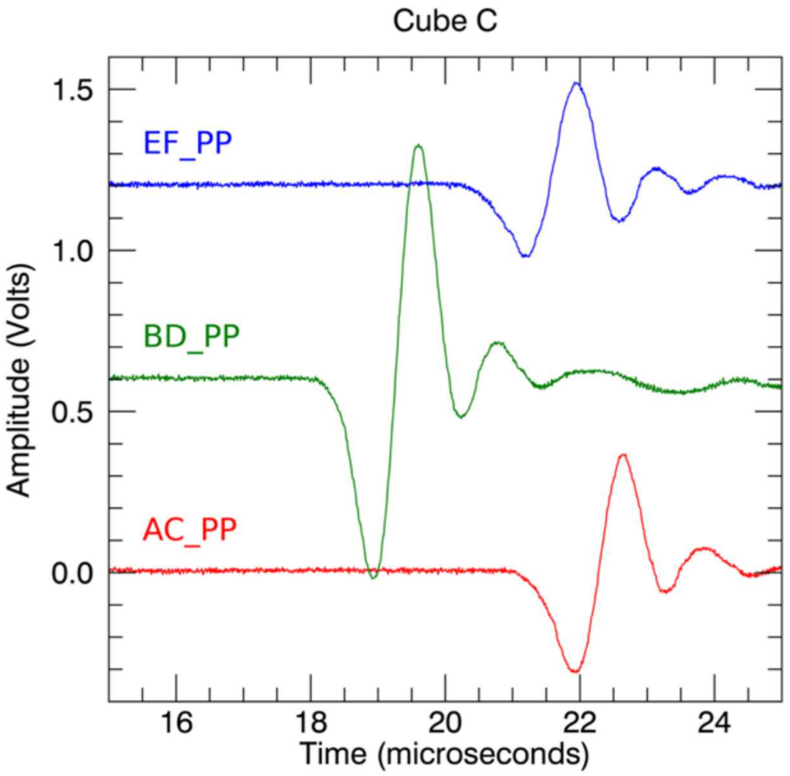

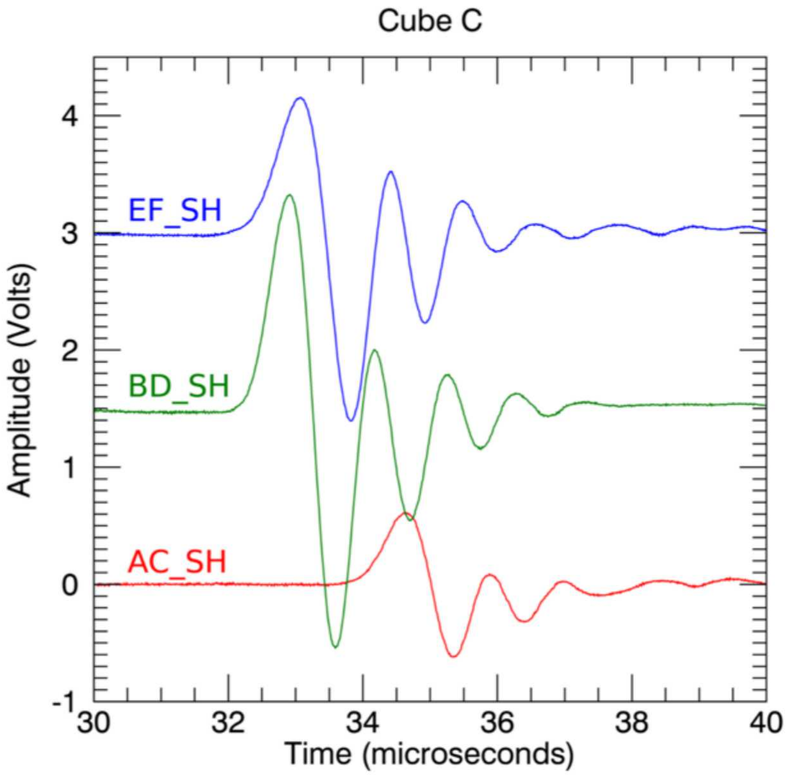

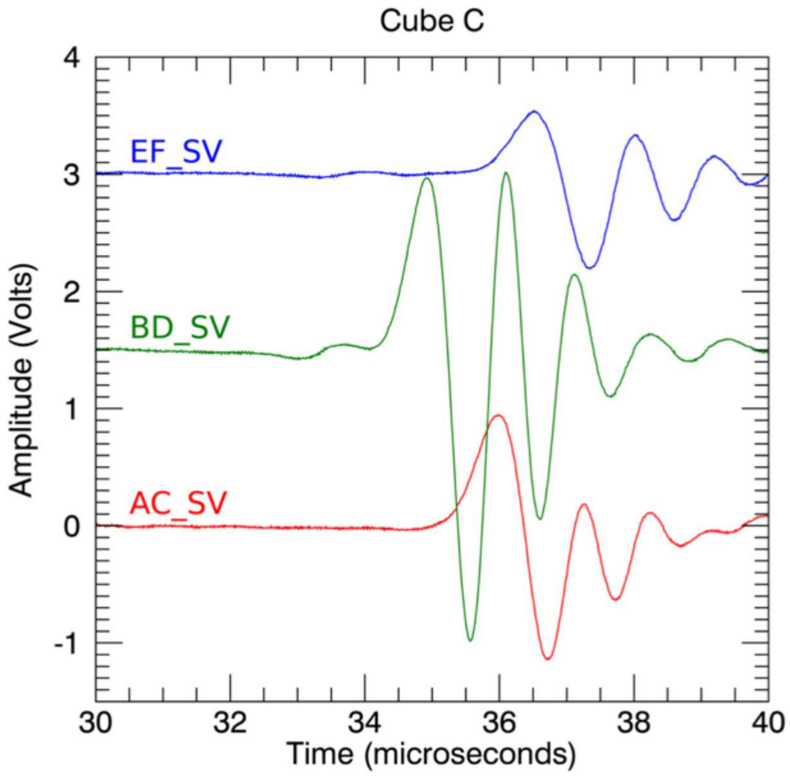

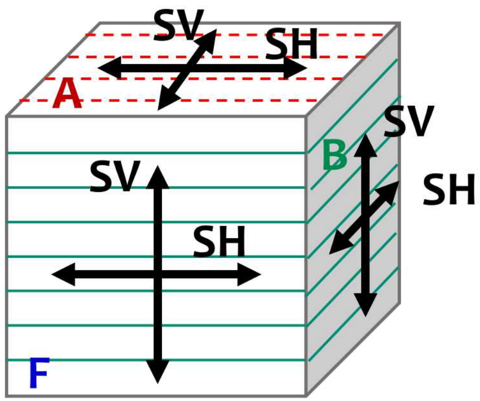

Polarization relative to layering

Wave Velocity for 3D Printed Samples

Compressional

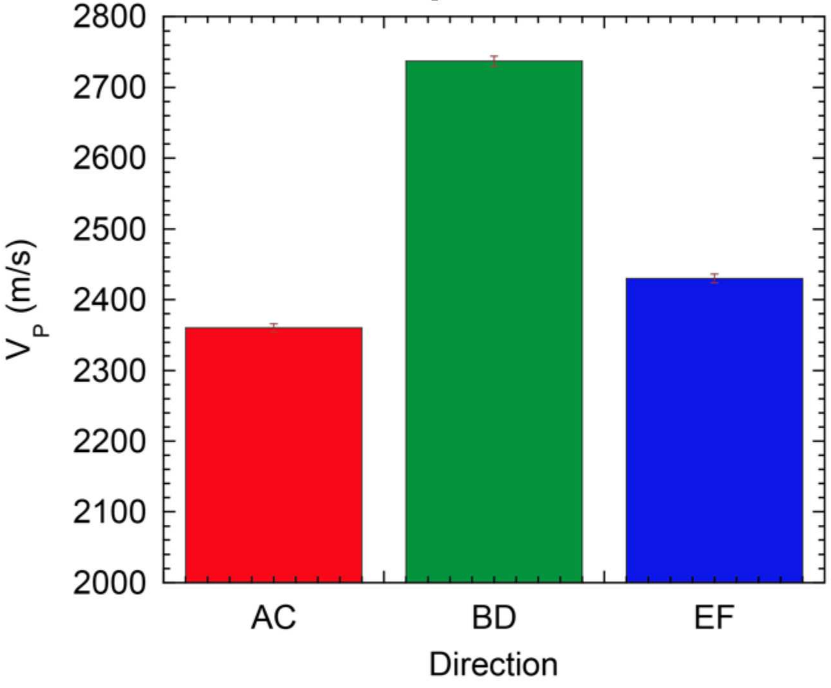

Shear Parallel to Layering

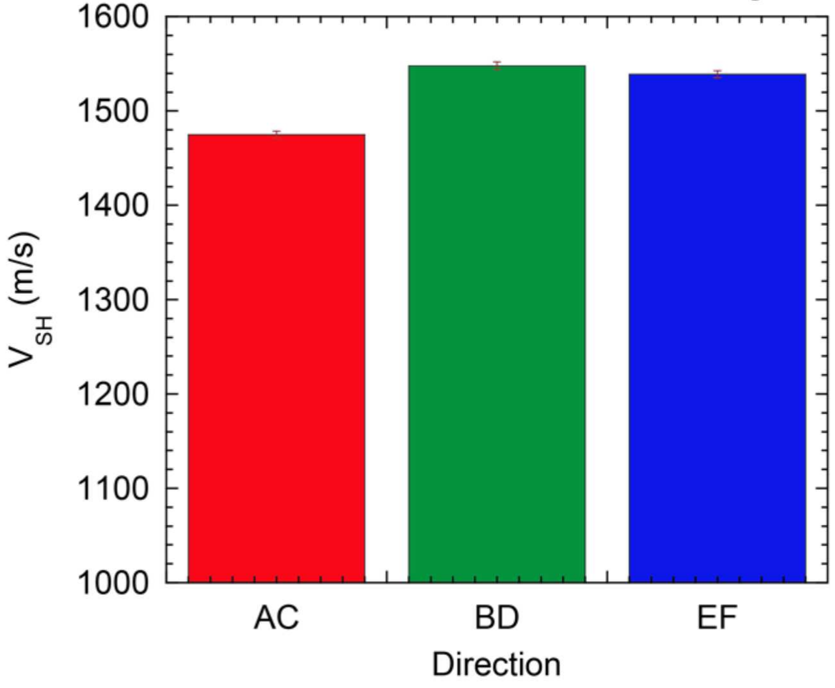

Shear Perpendicular to Layering

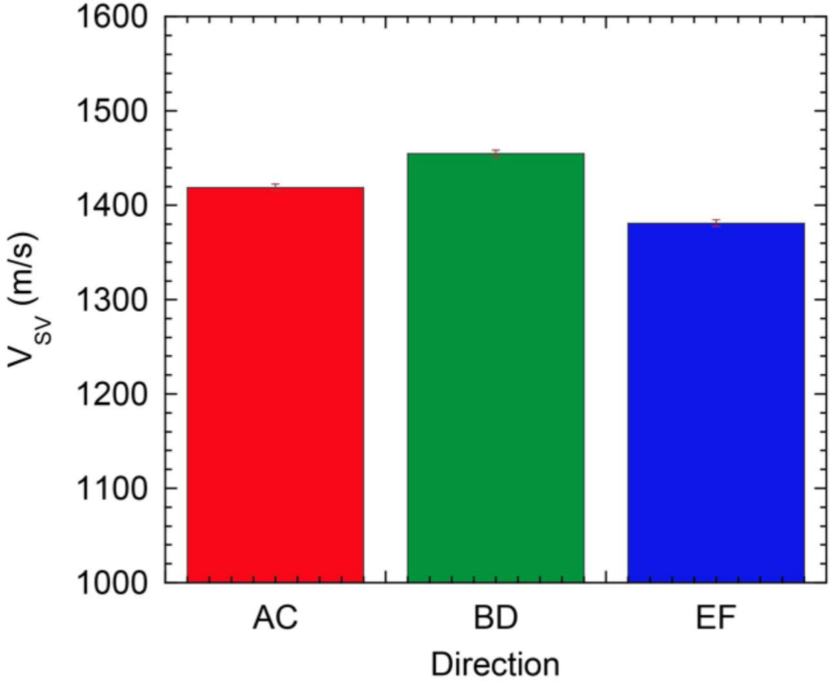

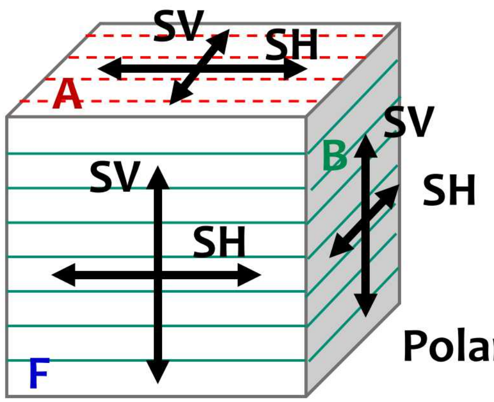

Polarization relative to layering

***With additional measurements elastic constants can be obtained**

Load-Displacement Behavior

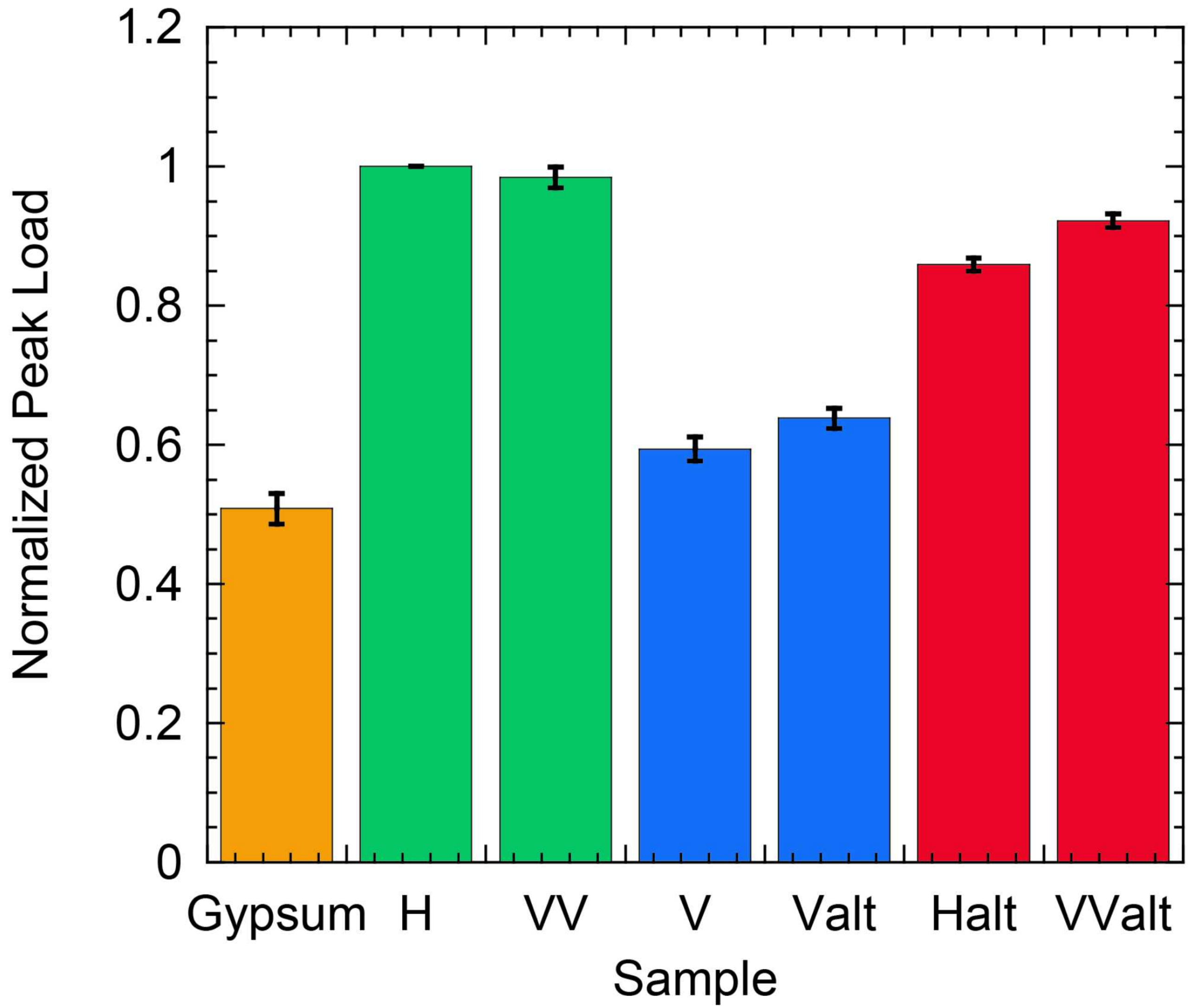

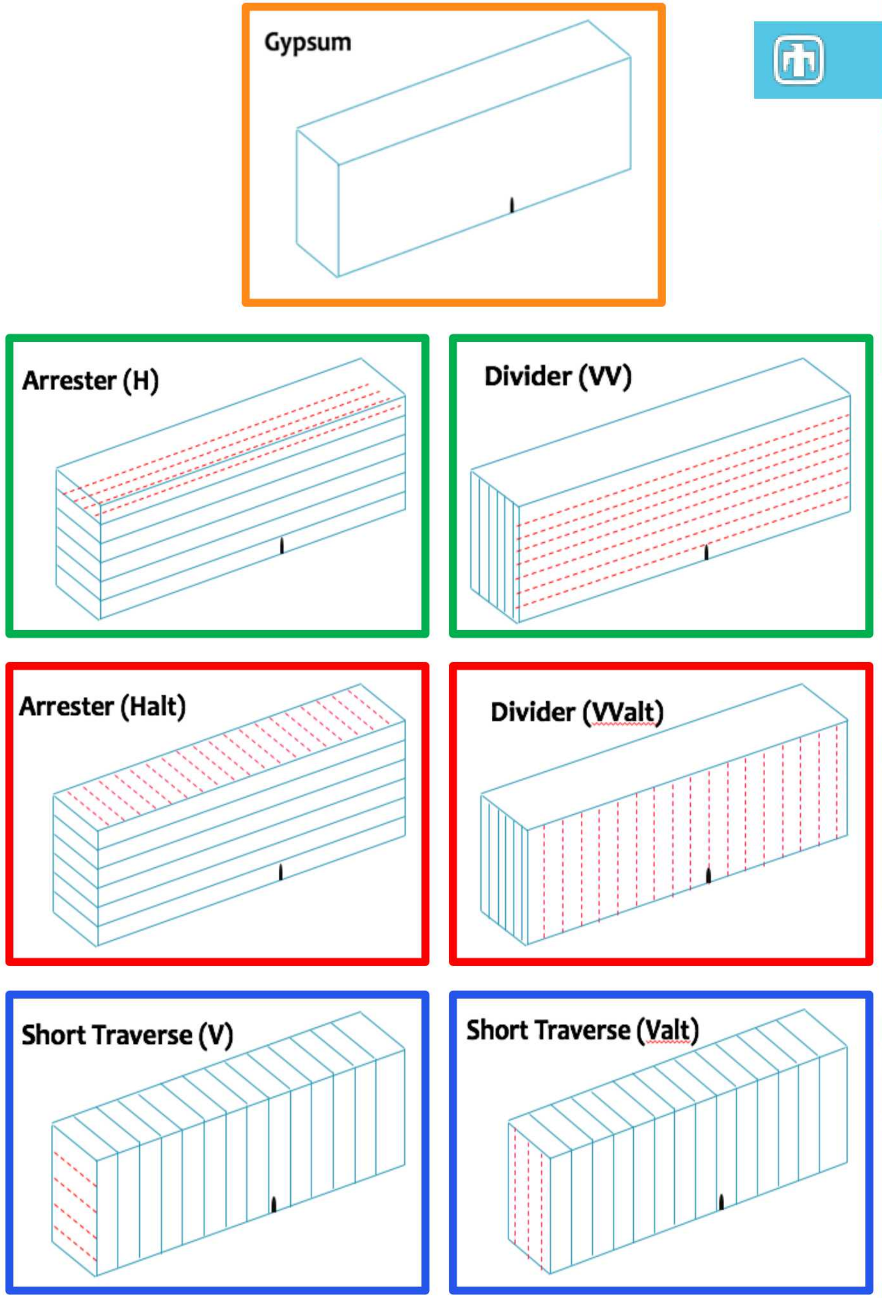

Fracture roughness and mineral texture

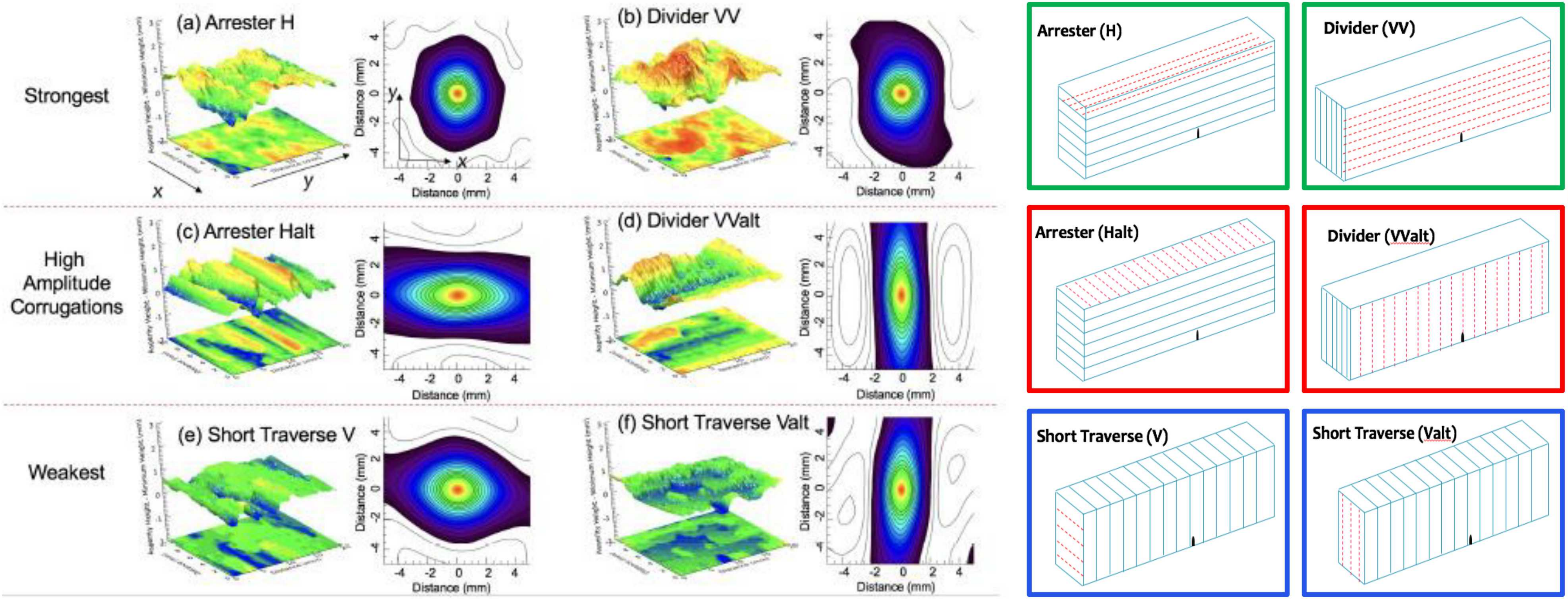

Jiang et al. (Sci Rep 2020, In press)

- Motivations
- Mechanical testing of Geo-architected rocks
- **Machine learning applications at laboratory scale**
- Machine learning applications at field scale
- Geological CO_2 storage
- Unconventional resources & recovery

Experimental Setup

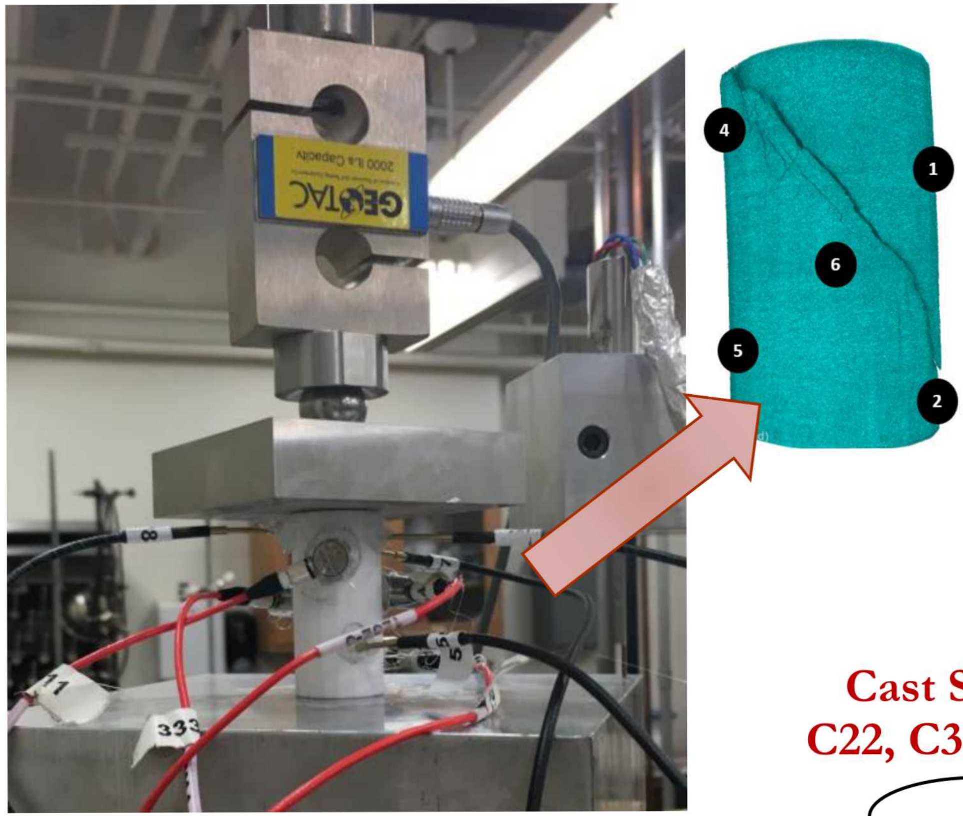

- Six sensors (Channels)
- 200-400 kHz filter to get rid of noise

Cast Sample
C22, C33, & C23

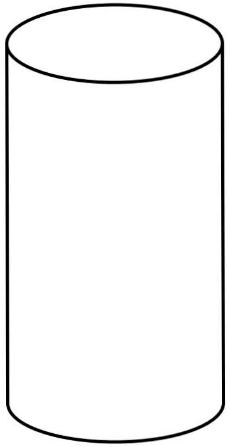

H Sample
dCH1, dCH2, & dCH3

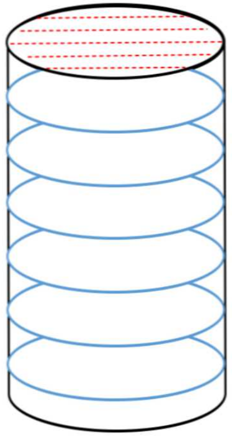

Acoustic Data

6 Samples → 2 Types of Samples → 6 Acoustic Channels Per Sample → 2 Different Frequency Ranges

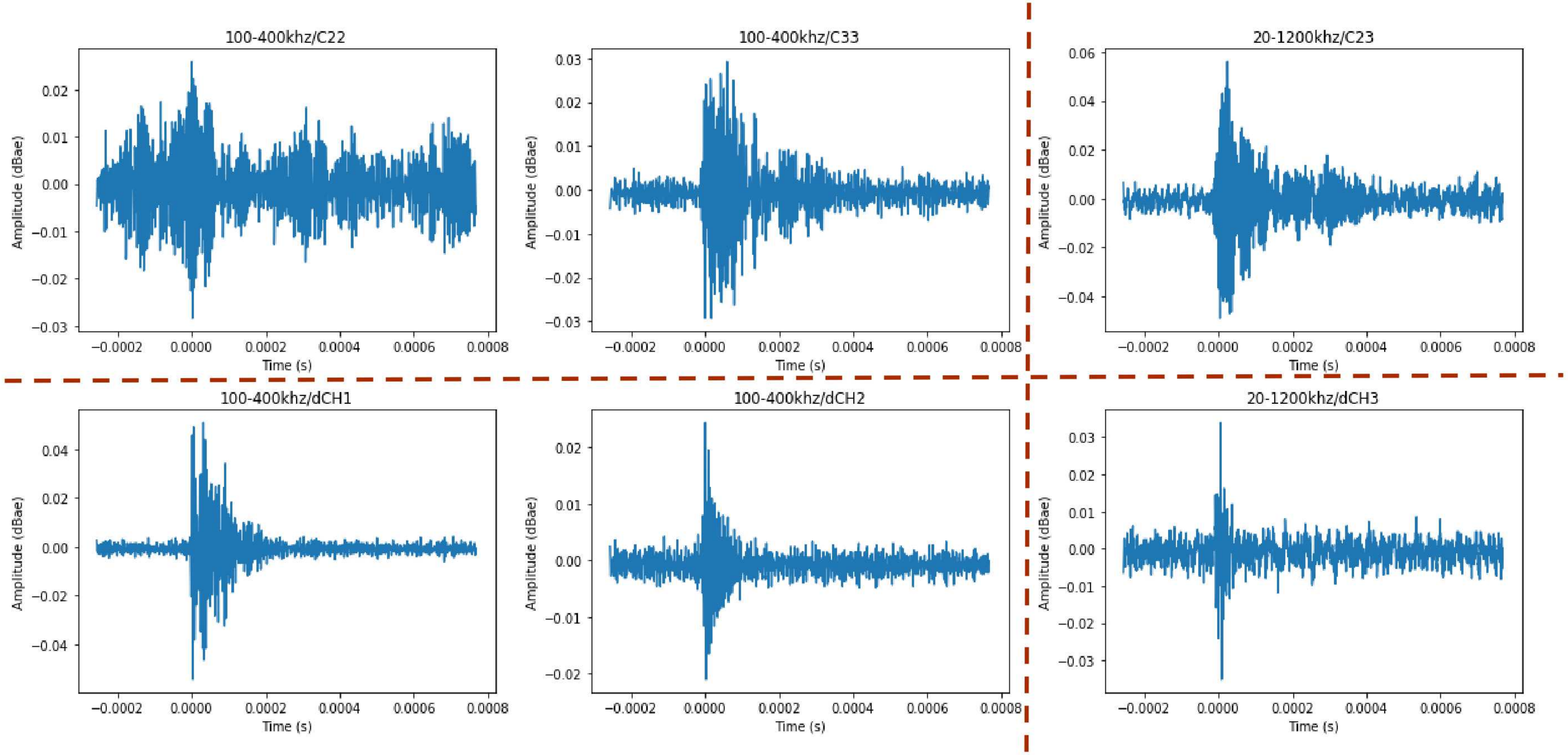

Acoustic Data

Goal:

1. Apply machine learning features to find patterns in the data.
2. Filter out noise to target significant events.
3. Identify precursors to failure.

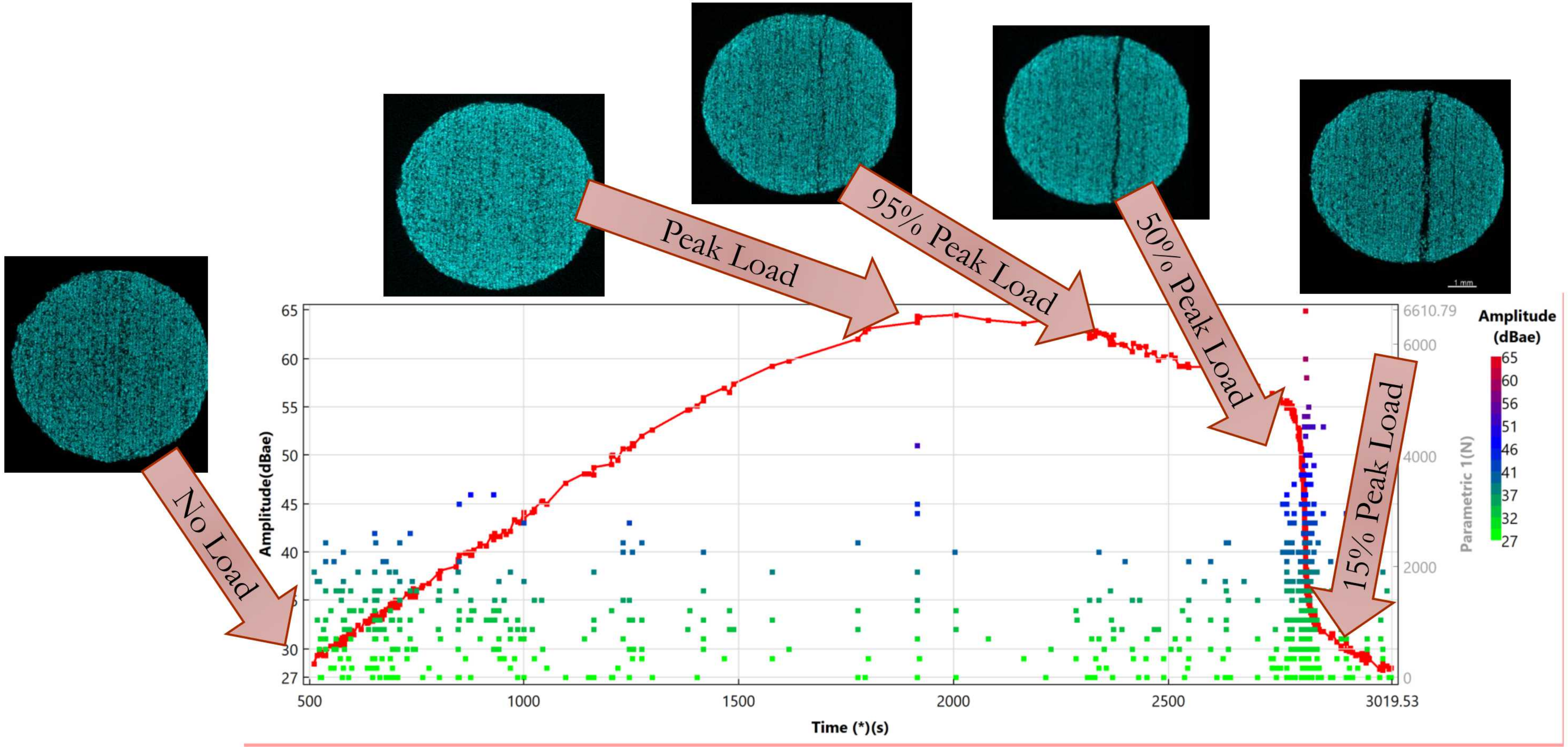

Simulations of crack initiation and acoustic emission

- 3 point bending with a central notch (2D, ABAQUS)
- Crack propagation and acoustic emission (XFEM)
- 6 sensor nodes sampling at 8 MHz
- 1-3 for training, 4-6 for testing
- Limestone material properties (homogeneous)

ML: fingerprint and K-means cluster (Holtzman et al. 2018)

- Clustering: acoustic state & mechanical state
- Spectrogram (Short Time Fourier Transform)
- Non-negative Matrix Factorization
- Hidden Markov Model (S states)
- K-means cluster

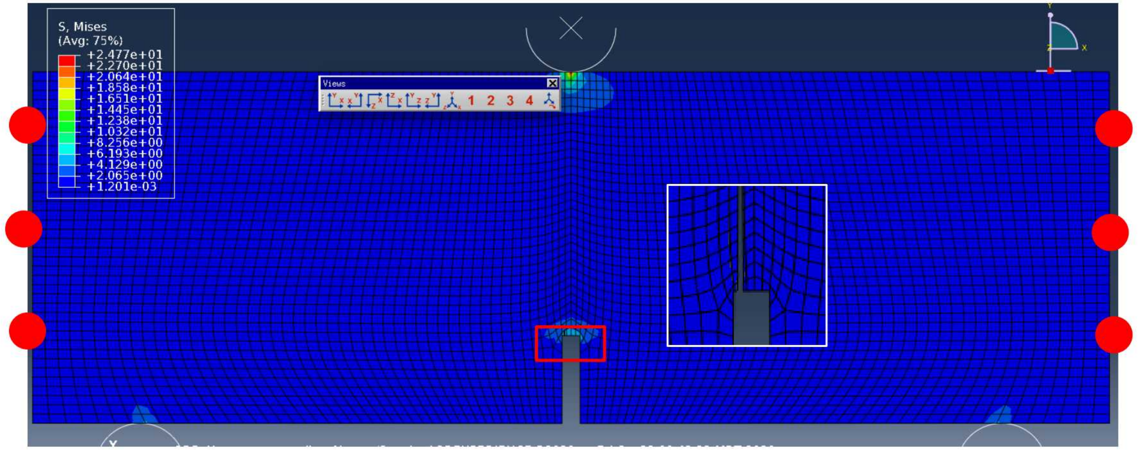

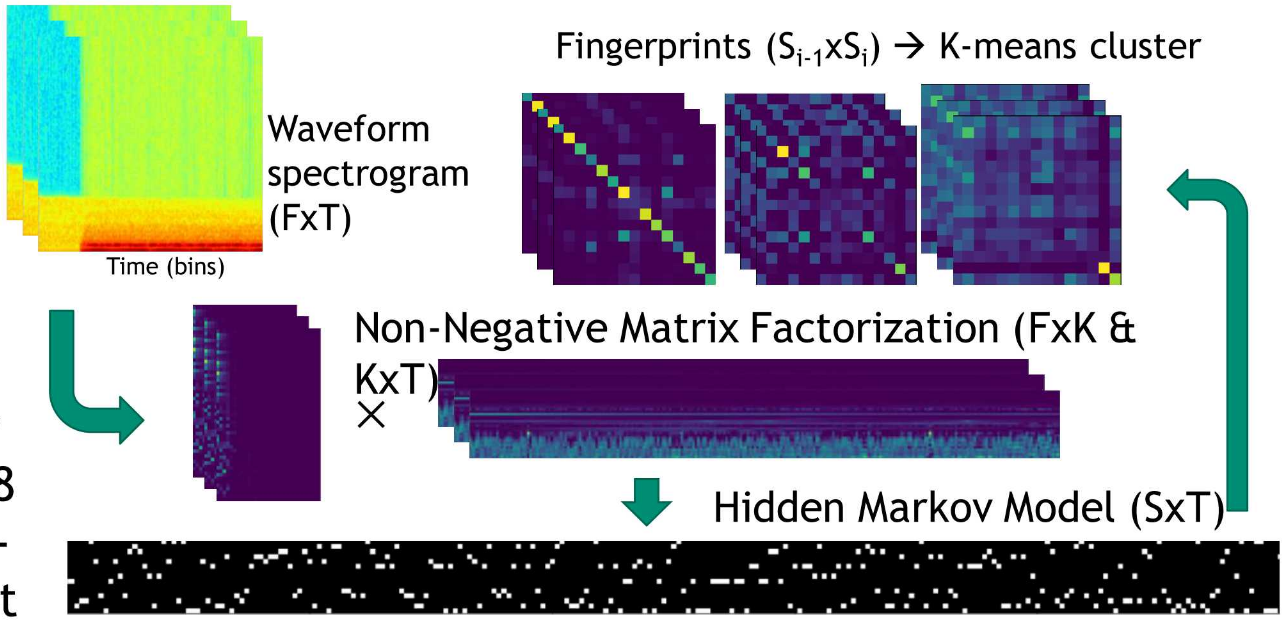

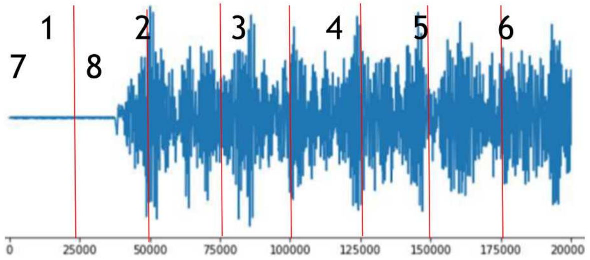

Acoustic state clustering by slicing simulated data into 8 window sets containing pre-crack (1), crack (2) and post crack (3-8) waveforms

Waveform Analysis for Machine Learning Applications

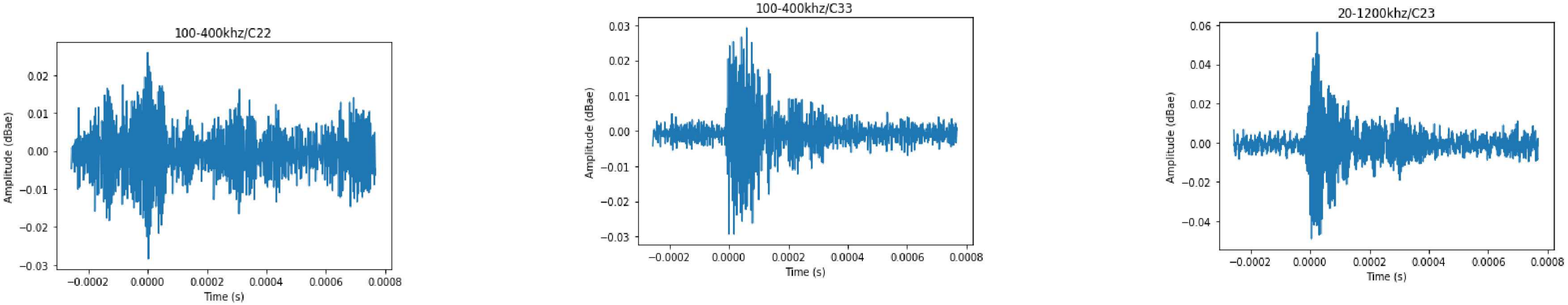

Waveform data is converted into a frequency domain (Spectrogram)

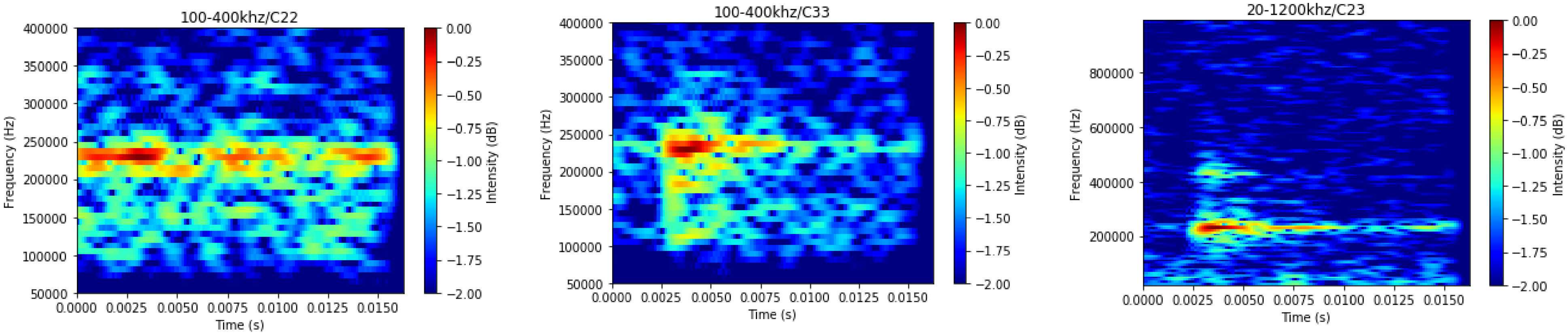

Machine Learning Applications for Waveform Analysis

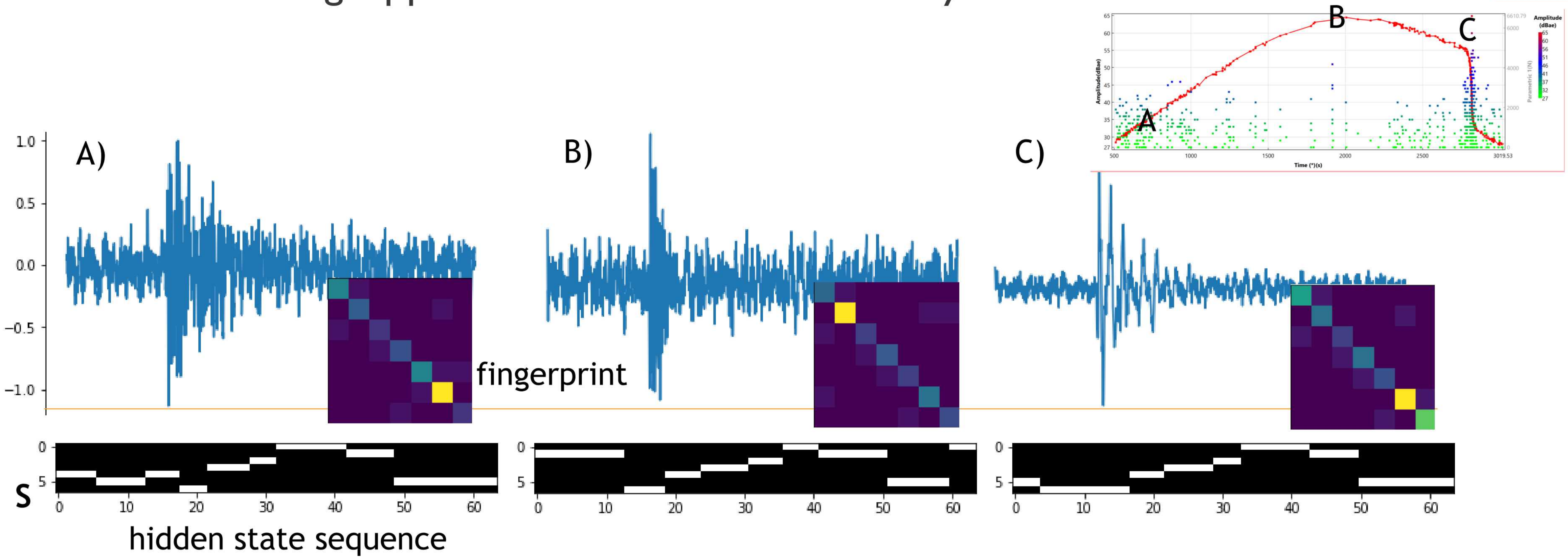

- Mechanical state clustering by comparing waveform evolution in the UCS test.
- Waveforms correspond to 3 stages in the loading curve, namely
- A) initial loading slope, B) max load region, C) post-failure region.

- Motivations
- Mechanical testing of Geo-architected rocks
- Machine learning applications at laboratory scale
- **Machine learning applications at field scale**
- **Geological CO_2 storage**
- Unconventional resources & recovery

Current Computational Approaches [DOE EFRC Project 2009-2018]

- Various numerical methods (e.g. finite element, finite difference, lattice Boltzmann) and experimental methods have been used to study multiscale, multiphysics processes (flow, reactive transport, mechanical deformation, etc) during carbon sequestration
- Next generation scientific computing (e.g. exascale high performance computing) and new waves of machine learning and artificial intelligence change the landscape for simulating complex, dynamic, and non-stationary processes
- Realtime forecasting of CO_2 flow, pressure propagation, and induced seismicity

High Fidelity Pore Scale Reactive Transport Experiments and Modeling

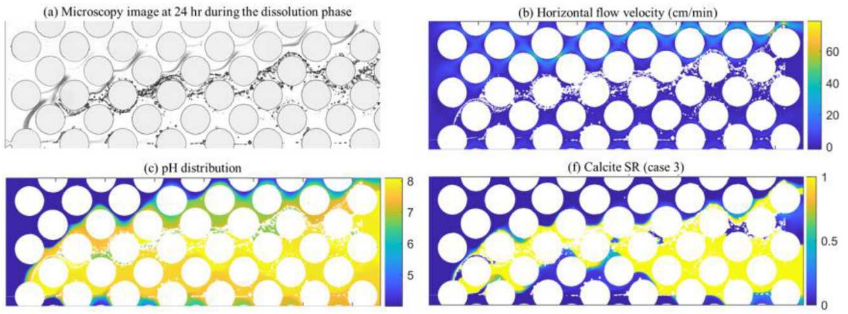

Yoon et al. (2012 WRR, 2015 RiMG, 2019 ES&T)

CO_2 gas phase flow in a water saturated sand box

Sand packing | CO_2 gas saturation | Sierra/Aria | PFLOTRAN | MIP

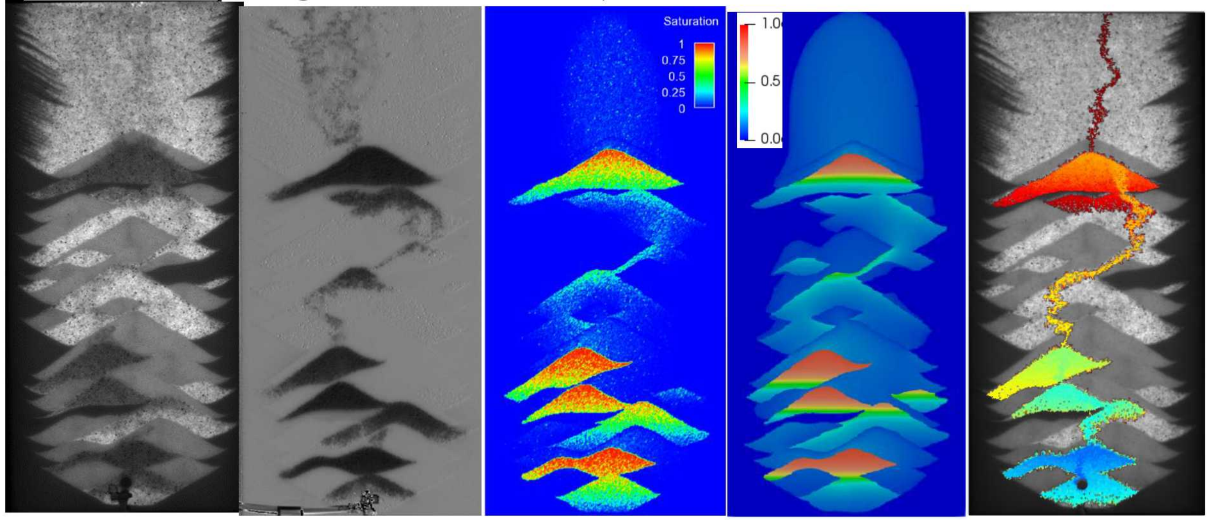

Coupled multiphase flow and mechanical deformation

(Sierra/Aria-Solid Mechanics, Martinez et al., 2017, Newell et al. 2017)

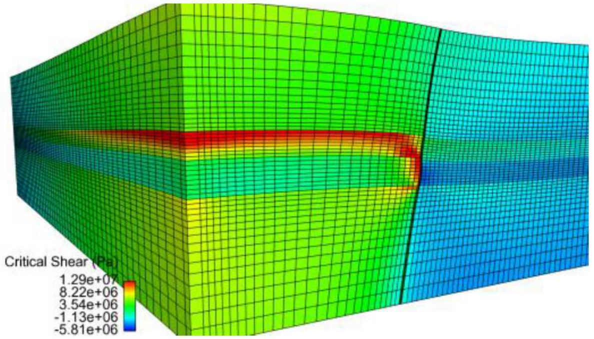

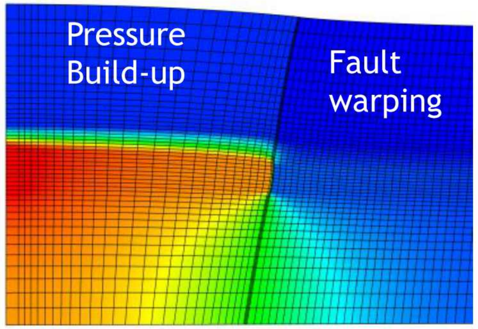

Poroelastic coupling effect on injection-induced seismicity

• Poroelastic coupling

- Stress equilibrium equation

$$\nabla \cdot [G(x)\nabla u] + \nabla\left[\frac{G(x)}{1-2\nu(x)}\right]\nabla \cdot u - \boxed{\alpha(x)\nabla p} + f = 0$$

- Inhomogeneous diffusion equation

$$S(x)\frac{\partial p}{\partial t} - \frac{1}{\eta}\nabla \cdot [k(x)\nabla p] = \boxed{-\alpha(x)\frac{\partial}{\partial t}(\nabla \cdot u)} + Q(x,t)$$

- Full poroelastic coupling is defined by ∇p in the equilibrium equation, acting as body forces in the stress equilibrium, and $\nabla \cdot u$ in the diffusion equation.

where S_i (Pa^{-1}) is the specific storativity and λ_i (Pa) and G_i (Pa) are the Lamé elastic parameters, and α_i (−) is the Biot-Willis coefficient representing the ratio of changes in the fluid volume to the total bulk volume for deformation at constant pore pressure. $\Lambda_i \equiv \kappa_i/\eta$ is the flow mobility, where κ_i (m^2) is permeability and η (Pa·s) is fluid

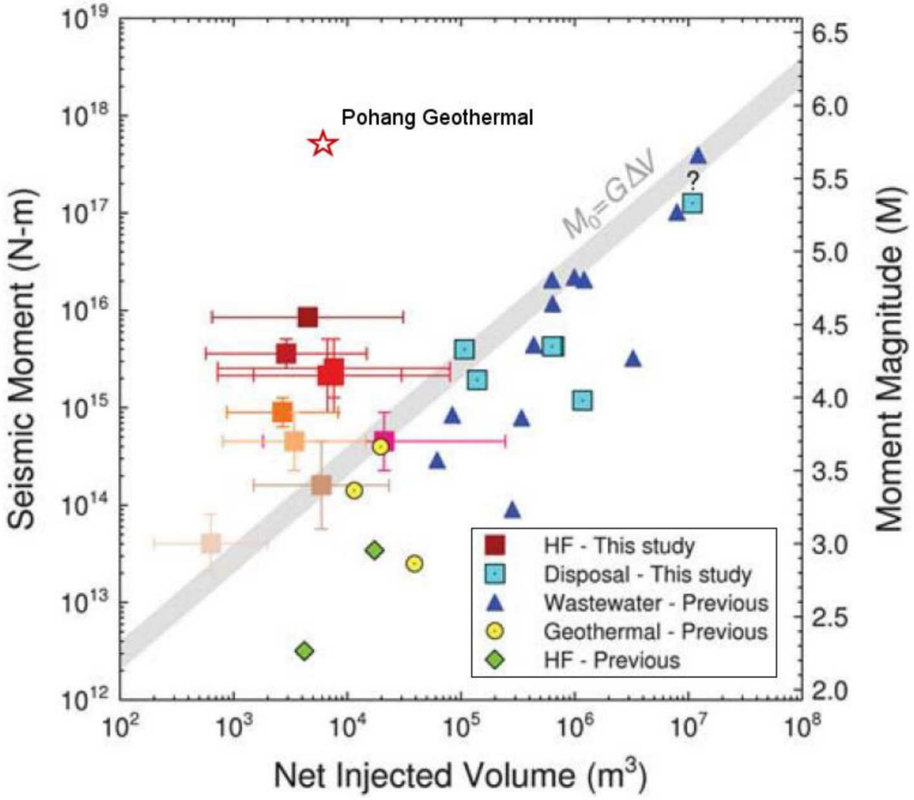

Atkinson et al. (Seism. Res. Lett., 631–647, 2016)

Chang, Yoon, & Martinez (BSSA, 2018), Chang and Yoon (JGR, 2018), Change et al. (Sci. Rep., 2020)

Poroelastic coupling effect on injection-induced seismicity

- ► Strike-slip fault(s) are modeled in a 2-D horizontal domain
- ► Injection for 5 days with the rate of 0.1 [kg/m/s] and then shut in to evaluate post shut-in behaviors
- ► Coulomb stress change ($\Delta\tau = f\Delta p + (\Delta\tau_s + f\Delta\sigma_n)$) from the initial stress state is obtained

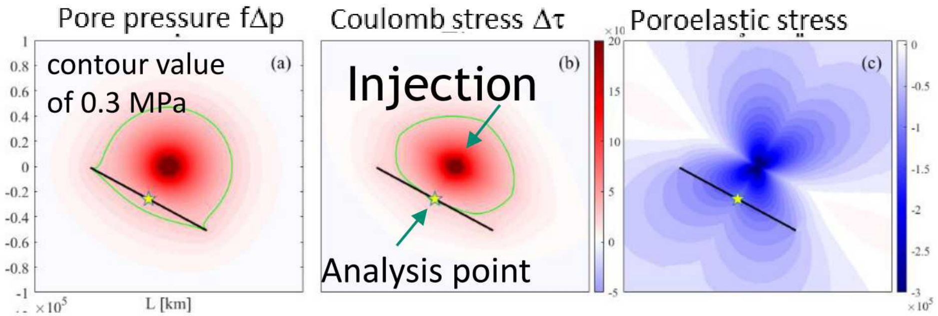

Mechanism of poroelastic behavior

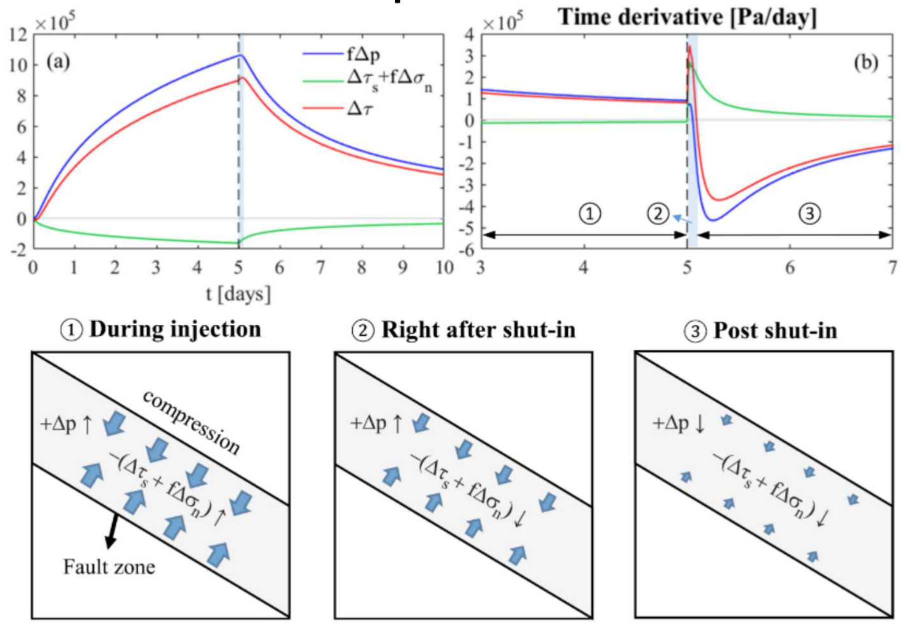

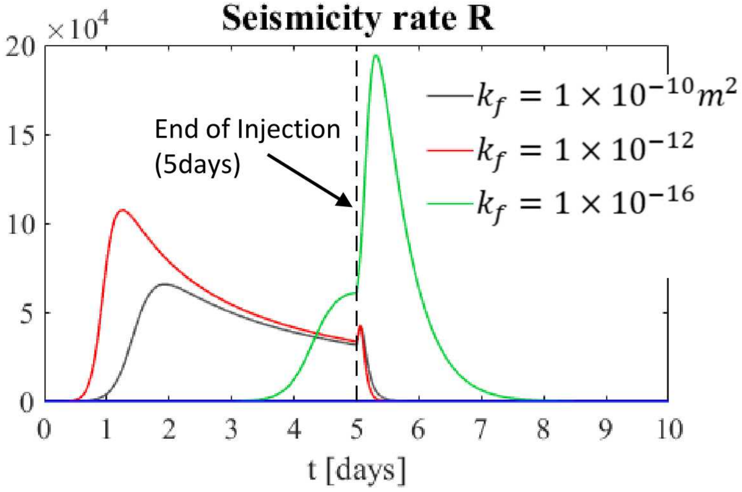

The moderately high-permeable fault (green) experiences significant increases in the seismicity rate (R) after shut-in because of combining effect of pore-pressure diffusion and poroelastic stressing.

Coulomb stress change

$$\Delta\tau = \underbrace{(\Delta\tau_s + f\Delta\sigma_n)}_{\text{Poroelastic stress}} + \underbrace{f\Delta p}_{\text{Pore pressure}}$$

$\Delta\tau_s$ = shear stress change
$\Delta\sigma_n$ = normal stress change
Δp = pore pressure change
f = failure friction coefficient

- (+) values of each quantity imply that the fault plane is moved closer to failure

Seismicity rate estimate

$$\frac{dR}{dt} = \frac{R}{t_a}\left(\frac{\dot{\tau}}{\dot{\tau}_0} - R\right)$$

t_a = characteristic decaying time

- R is the seismicity rate relative to an assumed prior steady-state seismicity rate at a background stressing rate

Integration of Machine Learning with Fundamental Studies and Field Scale Data

MicroCT imaging and flow and mechanical simulations of CO_2 flow

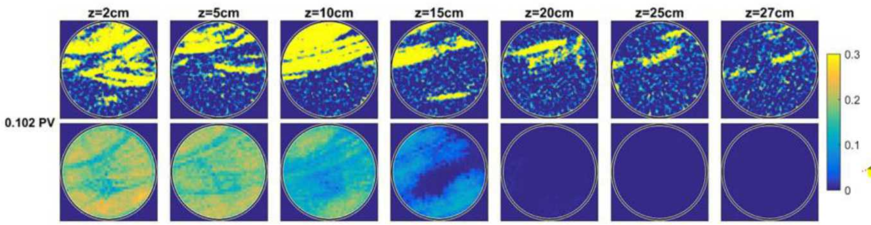

Krishnamurthy et al. (2017, JPSE)

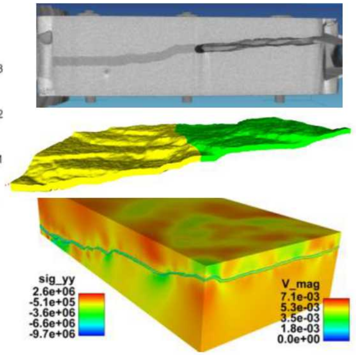

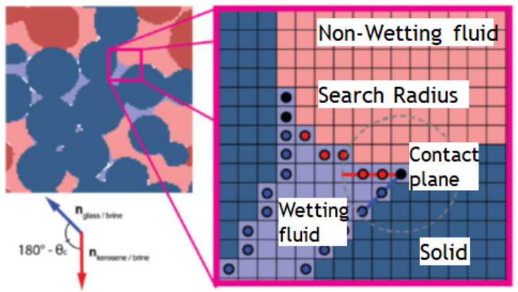

Klise et al. (2016, AWR)

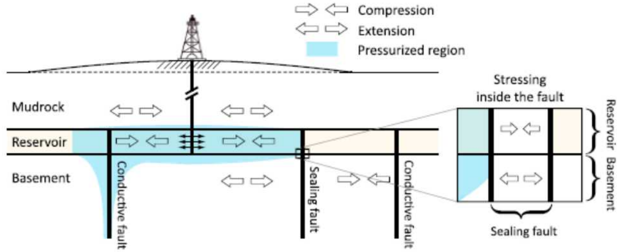

Chang and Yoon, JGR 2018

Fundamental Studies

Field Laboratories

Data-Driven Approaches

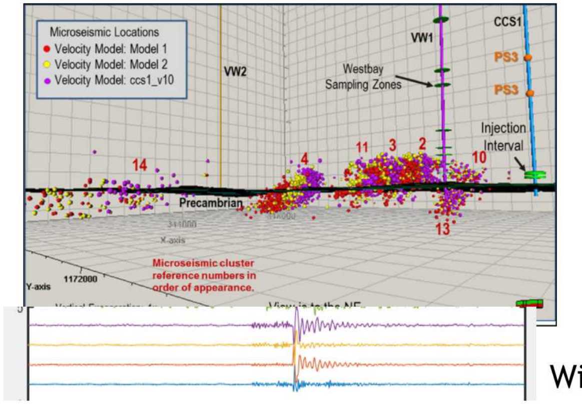

Will et al., IJGGC 2016

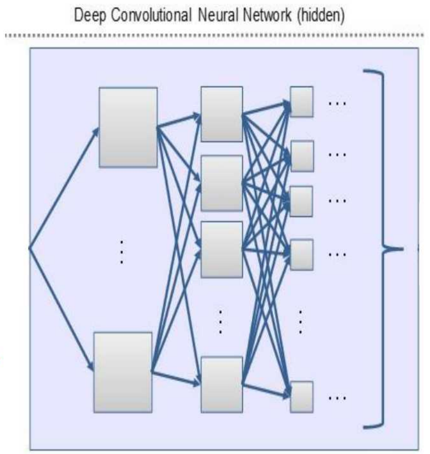

Realtime Forecasting of CO_2 Storage with Realtime Data Integration

DOE SMART Initiative:

Science-informed **M**achine Learning to **A**ccelerate **R**eal **T**ime (SMART) Decisions in Subsurface Applications

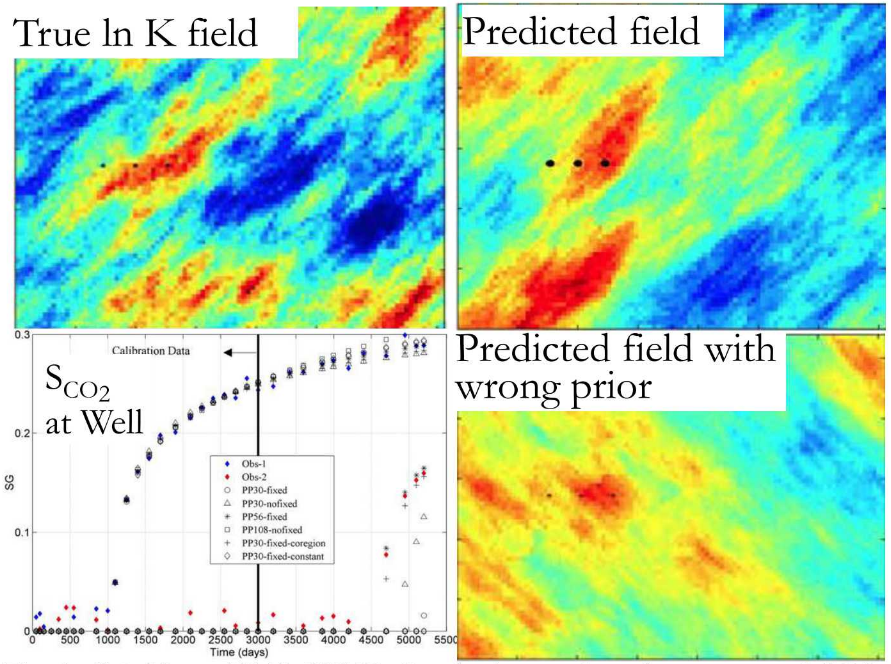

Tavakoli & Yoon (2013, WRR), Synthetic case based on an actual CO2 injection pilot test in Cranfield, MS

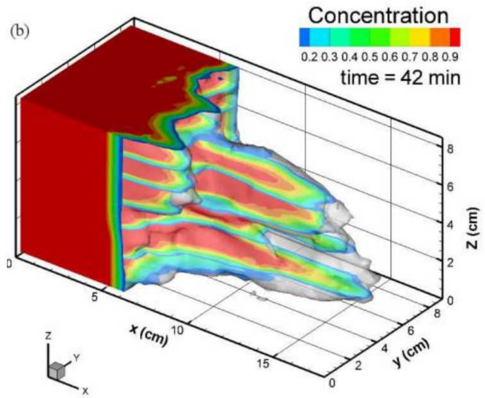

Yoon et al. (2008, 2013, WRR)

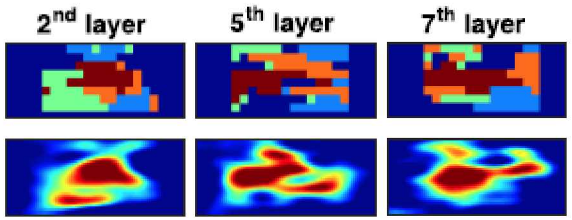

Lee, Yoon et al. (2016, WRR), 3D MRI Continuous spatial-temporal tracer experimental data (>2 million concentration data). Scalable subsurface inverse modeling of "big" dataset using "Jacobian-free" geostatistical inversion method

- Accurate prediction of CO_2 saturation at a monitoring well
- All algorithms are unable to correct the structural orientation of the permeability field using only the sparse dynamic data from wells, suggesting that **structural uncertainty should be incorporated into prior information**

Sandia ML task for the SMART Initiative:

- Large-scale hierarchical Bayesian inversion coupled with ML classifiers (e.g., fuzzy logic or random forests) or high-dimensional input-output relationships with deep-learning neural networks (e.g., convolutional neural networks, recursive neural networks)
- Data-driven modeling of CO_2 flow and pressure prediction with realtime data integration
- Virtual learning tool development

Machine learning applications for fault detection and the presence of hidden faults/fracture networks (in collaboration with ISGS and MIT)

- Improve the detection of low-magnitude, unidentified events & locations to discover undetected/hidden fault/fracture systems
- Rapid recognition of the presence of faults/fault interactions
- Characterize microseismic waveforms, the relations among the events, and reliable identification of microseismic sources integrated with forward/inverse modeling

Target clusters 2 & 4
Two 2-months data

Illinois Basin Decatur Project

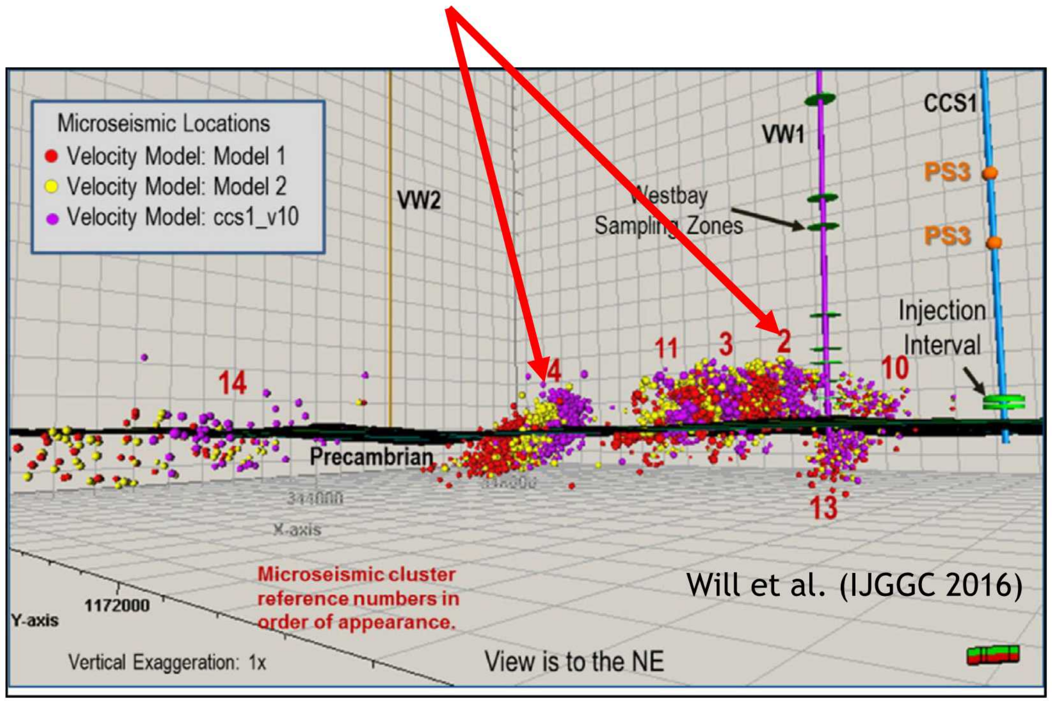

Will et al. (IJGGC 2016)

- Raw continuous data (100's TBs) – 10s windows
- Detected event data (~19K data) – 2s windows
  ↓ manual selection
- Located event data (~5K data) - 2s windows

Various machine/deep learning approaches for microseismic data

- Supervised ML: Convolutional neural network (CNN) for event detection and location
  - Open source ConvNetQuake (Perol et al., 2018)
    - Processed data from ISGS will be used to train models
    - Trained model will be used to validate again the remaining dataset to develop real-time recognition of events and locations
- Unsupervised ML: Waveform similarity-based event detection methods & Hidden Markov Model & clustering
  - Fingerprint and Similarity Thresholding (FAST, Stanford FAST group)
    - FAST shows the increase in event detection of low magnitude seismicity by > a factor of 10
    - High efficiency in big data processing time
  - Dimension reduction (Non-negative matrix factorization), Hidden Markov model, & clustering
    - Distinctive waveform pattern in spectral domain
- Template matching (EQcorrscan)
  - This is a refence case whose results will be compared with ConvNetQuake and FAST for efficiency and interpretability
- Characterization of Microseismic events
  - Spectral clustering and regression-based machine learning analysis (e.g. random forest)
    - Identify seismic phases from successive slip or fracturing stage events and their constitutive wave patterns
    - Extract the salient features present in the data set, such as individual wave types, spectral content, p-s converted waves, and local energy decay
    - Link microseismic data to other measured/simulated quantities (e.g., pressure and stress field)

ConvNetQuake CNN Architecture
Perol et al. (2018, SciAdv 2018)

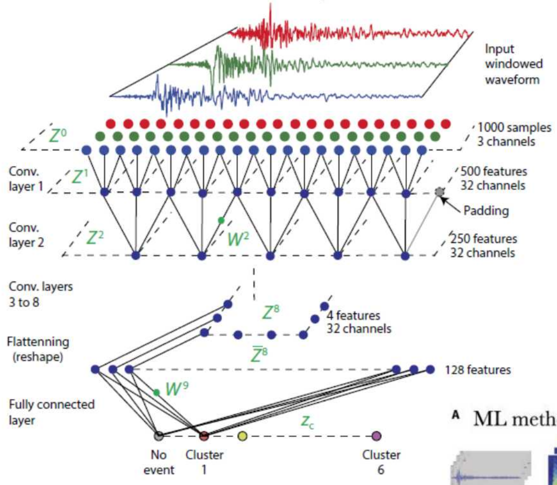

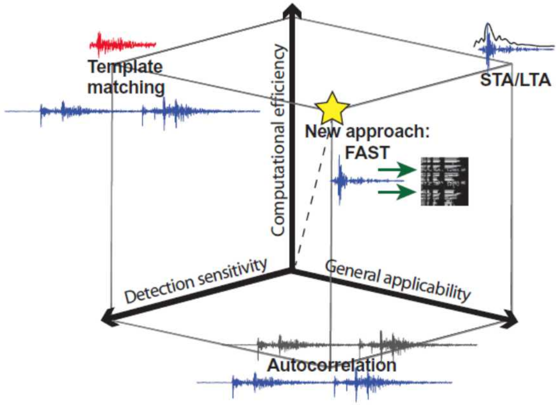

Earthquake detection methods from C.E. Yoon et al. (SciAdv 2015)

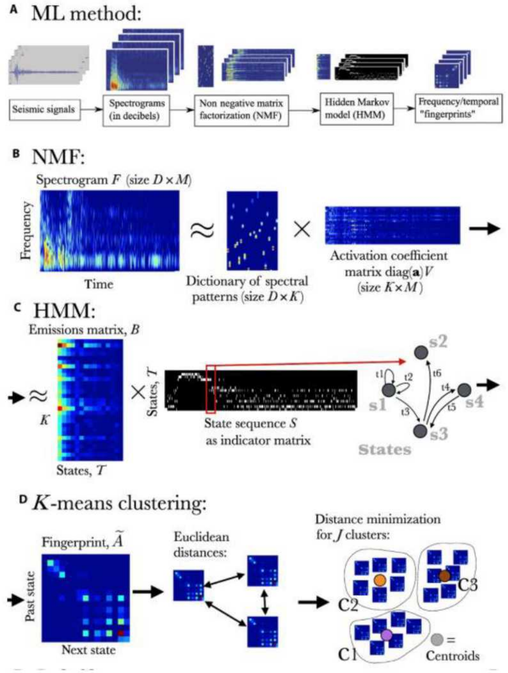

Holtzman et al. (2018, SciAdv)

Thank You!